

SUPPLEMENTARY REPORT

STATIC INFLATION TEST

B.1.1.1.1.1.1

December 1963

Prepared Under

Contract No. NAS 5-378

Report No. 0038-S-7

FOR

National Aeronautics

And Space Administration

N67-85064

(ACCESSION NUMBER)

70

(PAGES)

CR-87028

(NASA CR OR TMX OR AD NUMBER)

(THRU)

(CODE)

(CATEGORY)

Conductron



Corporation

343 SOUTH MAIN STREET ANN ARBOR, MICH.

SUPPLEMENTARY REPORT  
STATIC INFLATION TESTS  
BALLOON #16

DECEMBER 1963

Prepared for:  
NATIONAL AERONAUTICS AND SPACE ADMINISTRATION  
Goddard Space Flight Center  
Greenbelt, Maryland

Under:  
Contract No. NAS 5-3232

Report No. 0038-S-1

## INTRODUCTION

This report is concerned with the Radar Reflectivity Measurement performed by Conductron Corporation for NASA as part of the Static Inflation Tests, Lakehurst, New Jersey, NAS, November - December 1963.

## MEASUREMENT REQUIREMENTS

On 18 December 1963, Echo II Balloon #16 underwent static inflation testing at the Lakehurst NAS dirigible hanger #1. The test model was a flight quality balloon and the test objective was to obtain radar reflectivity data as a function of inflation pressure. Measurements were to be made at frequencies of 1.70 Kmc and 5.45 Kmc, at vertical polarizations and as a function of continuous bistatic angle between  $0^{\circ}$  and  $30^{\circ}$ . One of the constraints which was placed on the reflectivity measurement system was that the measurement time was to be minimized. The effect of this requirement on the measurement equipment and procedure is discussed in the following sections.

## DESCRIPTION OF EQUIPMENT

The general layout of the measurement setup is shown in Figures 1 and 2. A scaffold 44 feet high was erected in the hanger, and a wooden track 87 feet long was constructed on top of the scaffold. The track formed a circular arc having a radius of 167.5 feet so that the track was approximately 100 feet from the surface of the balloon. The angle subtended by the arc was  $30^{\circ}$ . A pair of standard gain horn antennas, one L-Band and one C-Band, were mounted at either end of the track as shown in Figure 3. They were mounted side by side so that both were pointing at the balloon and aligned along the balloon radius. These horns were the transmitting antennas and were connected by coaxial cable to appropriate CW oscillators. The oscillators and their control circuitry were located on a platform immediately below the track, as shown in Figures 2 and 4.

A pair of receiving horns were mounted on a movable cart in a manner similar to the transmitting antennas. These are shown in Figure 5. They were connected by coaxial cable to two Scientific-Atlanta receiving systems which were located on the deck of the hanger in the console control center shown in

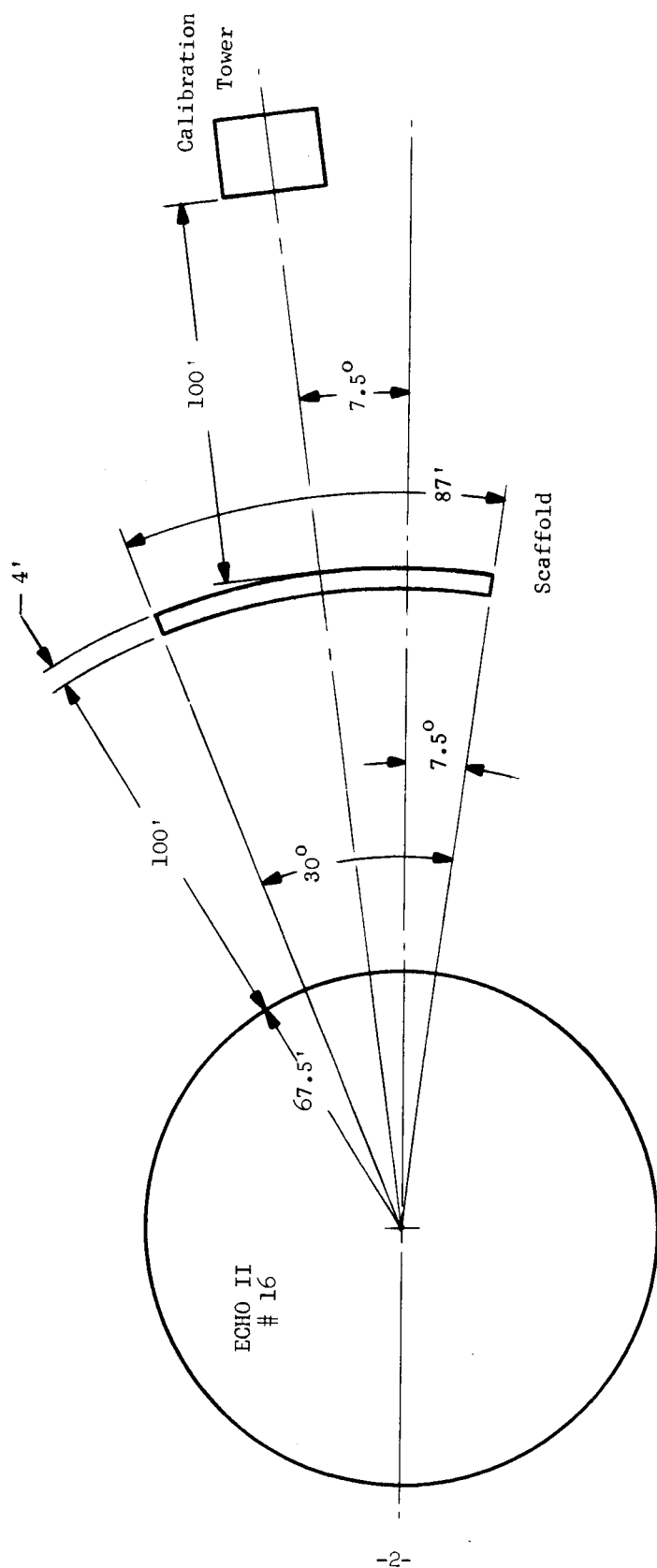


Figure 1 Plan View of the Measurement Setup



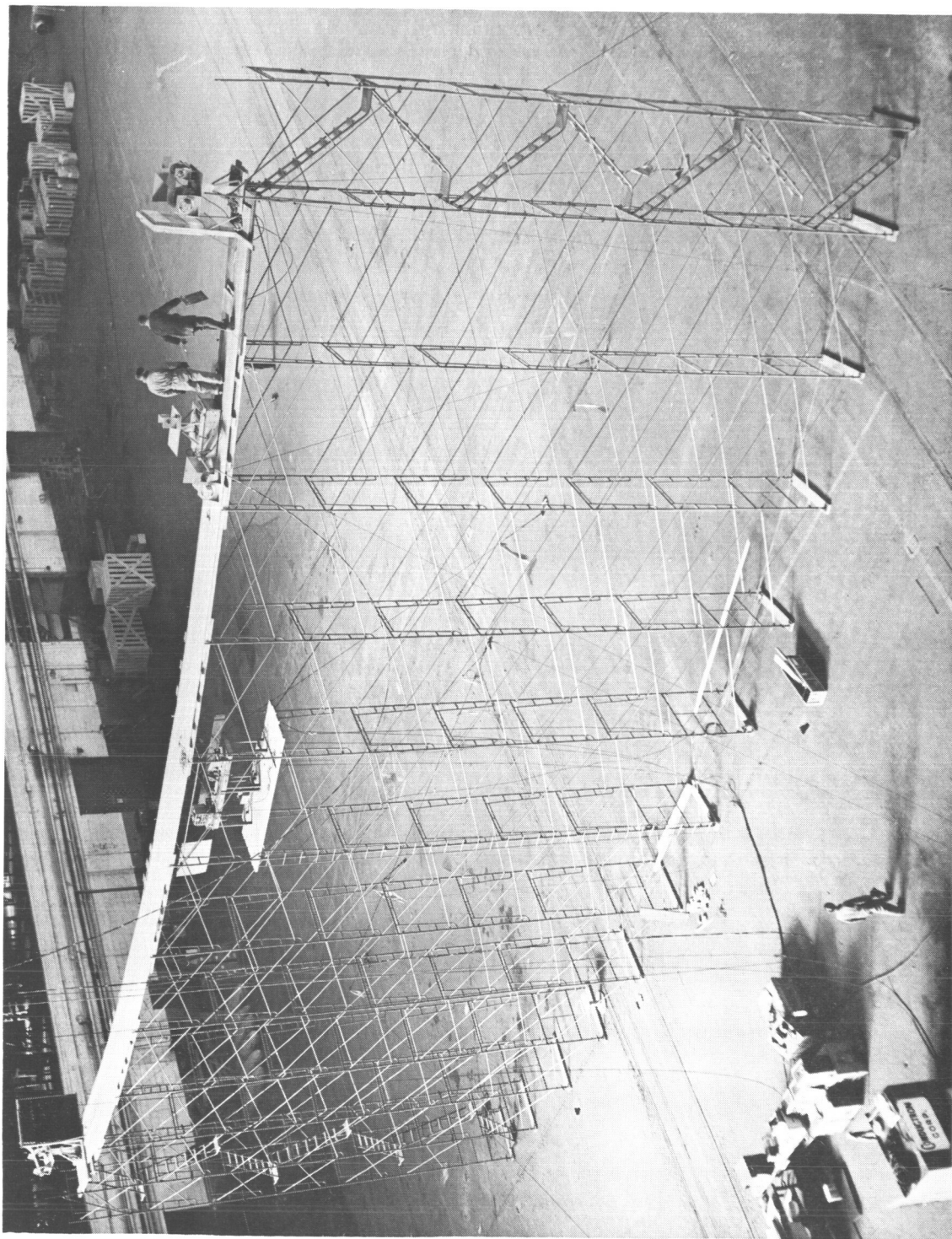


Figure 2

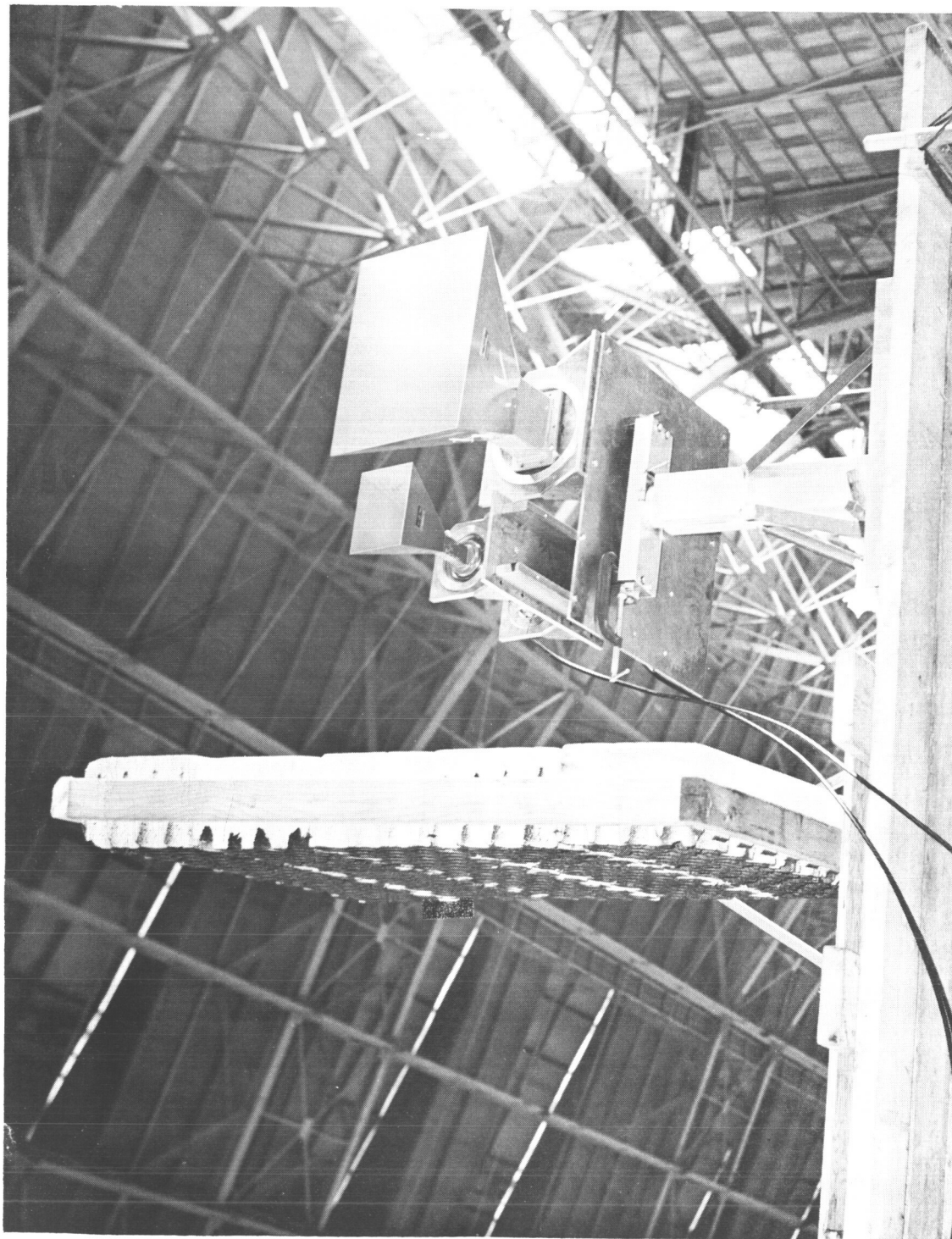


Figure 3

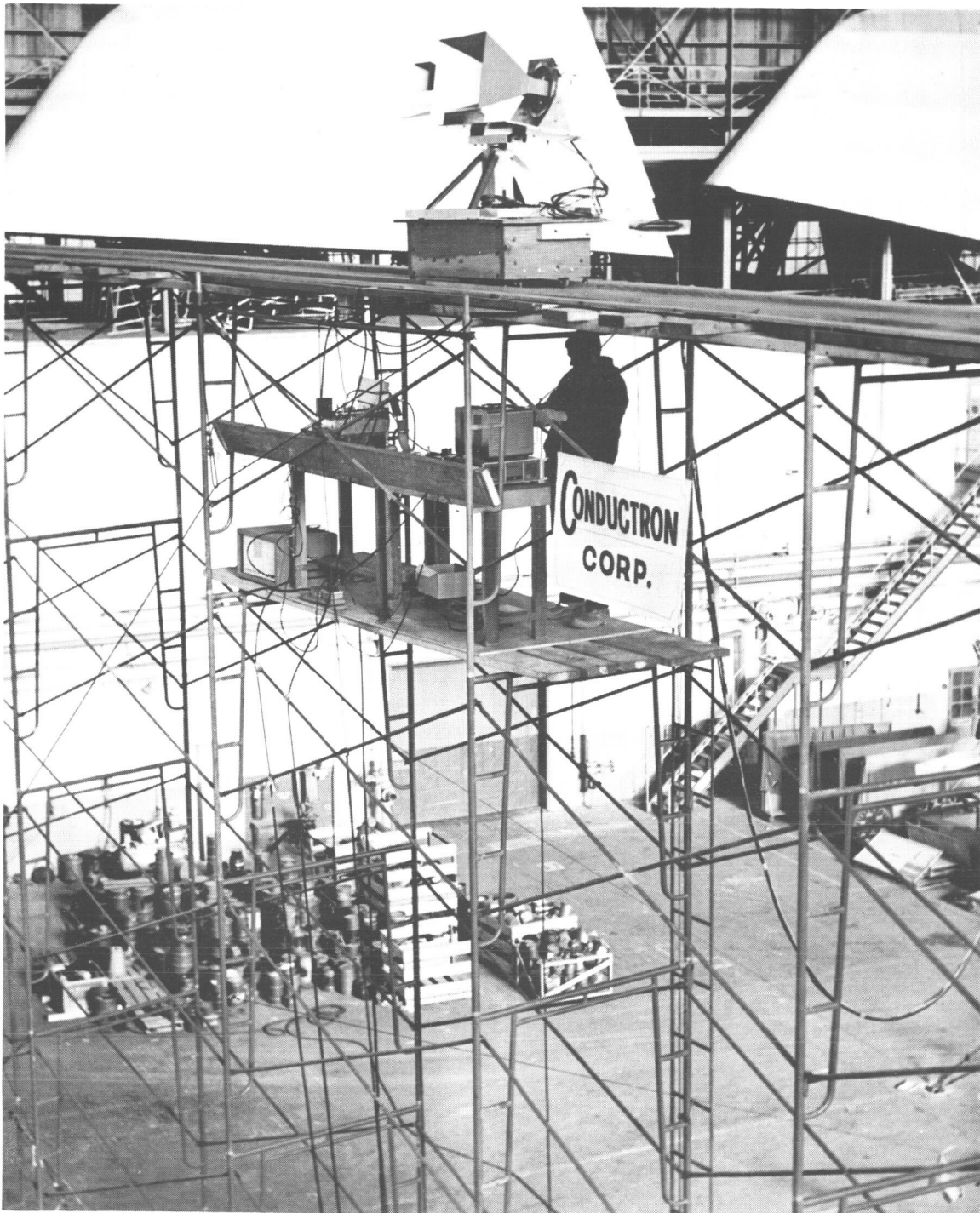


Figure 4





Figure 5

Figure 6. The receivers in turn were connected to two Scientific-Atlanta logarithmic chart recorders. The movable cart was equipped with a synchro transmitter which was also connected to the recorder. Thus, the data which were obtained were in the form of backscattered power as a function of bistatic angle. The coaxial cable connecting the receiving antennas to the receivers were arranged so that a constant cable length could be maintained regardless of the position of the cart on the track. A general block diagram of the transmitter and receiver systems are shown in Figure 7.

In accordance with the requirement for minimum measurement time, considerable effort was expended in the design of the cart and the antenna mounts. The purpose of the cart was to move along the track during a measurement sequence thus providing continuous reflection data as the bistatic angle was varied. It was equipped with a variable speed motor which was driven by a variac located at the console control center. Thus, the Measurement Test Director could increase the speed of the cart slowly to a maximum of 2.5 ft/sec so as to avoid extreme accelerations which might have resulted in misalignment of the receiving antennas. The antenna mounts incorporated provisions for angular adjustments in both azimuth and elevation and for small changes of antenna position in both the horizontal and vertical directions. In addition, in order to make the mounts as versatile as possible, provisions were included for rapid rotation of the polarization vector.

Calibration of the reflectivity data was accomplished by the use of "primary" and "secondary" calibration standards. The primary calibration standard was a rectangular flat plate having a physical area of  $0.928 \text{ m}^2$ . The radar cross section of this plate is  $25.4 \text{ db} > \text{m}^2$  at 1.70 Kmc and  $35.6 \text{ db} > \text{m}^2$  at 5.45 Kmc. The flat plate was mounted on top of a tower which was located on a line bisecting the arc subtended by the scaffold and 100 feet from the scaffold on the opposite side from the balloon. The mounting was accomplished using a Scientific-Atlanta model positioner having a synchro transmitter and capable of continuous azimuth rotation. The position of the flat plate was controlled remotely from the console control center. The tower on which the plate was mounted was covered with microwave absorber so as to prevent nullification of the calibration data by multiple reflections. A picture of the

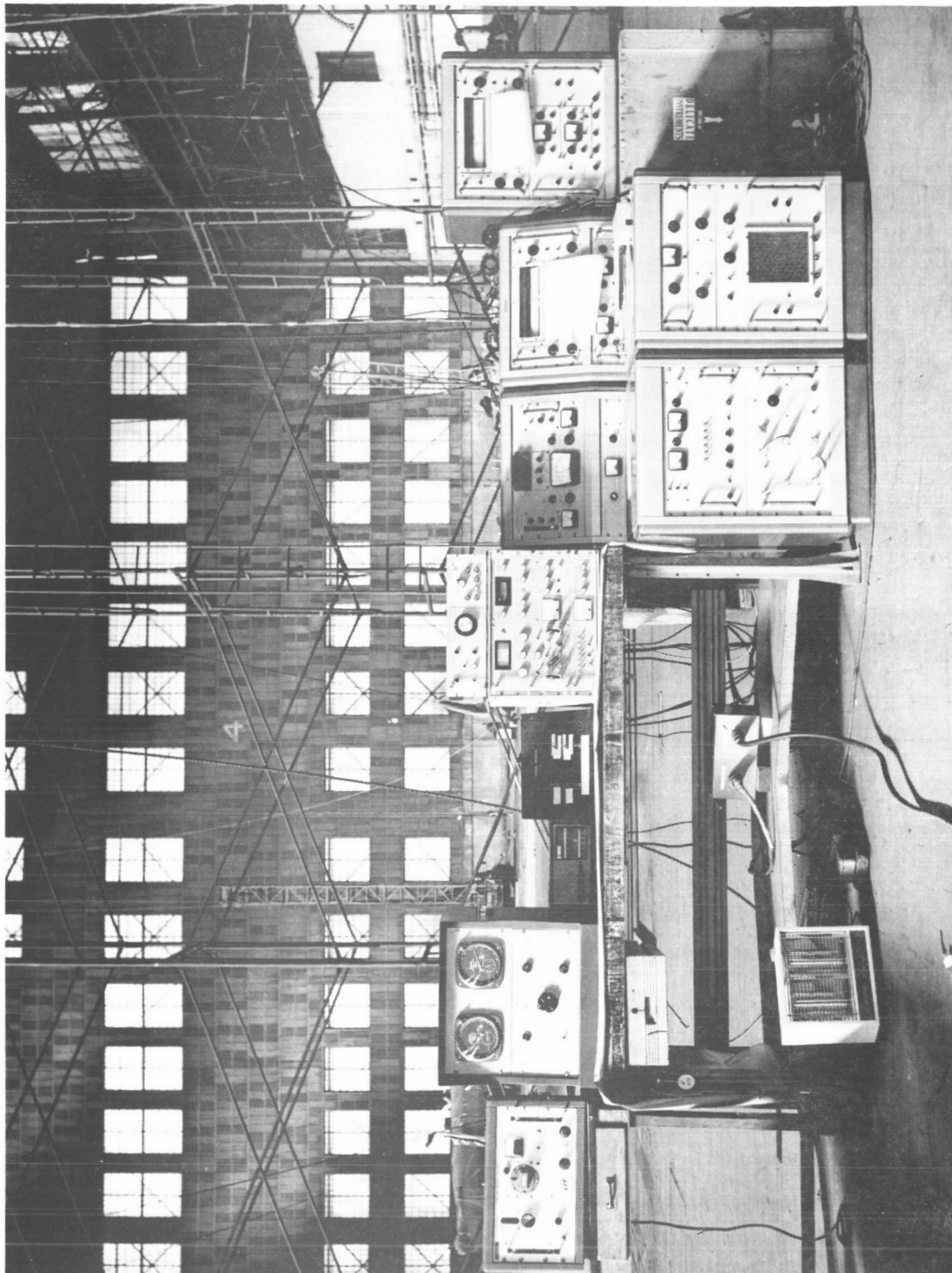


Figure 6

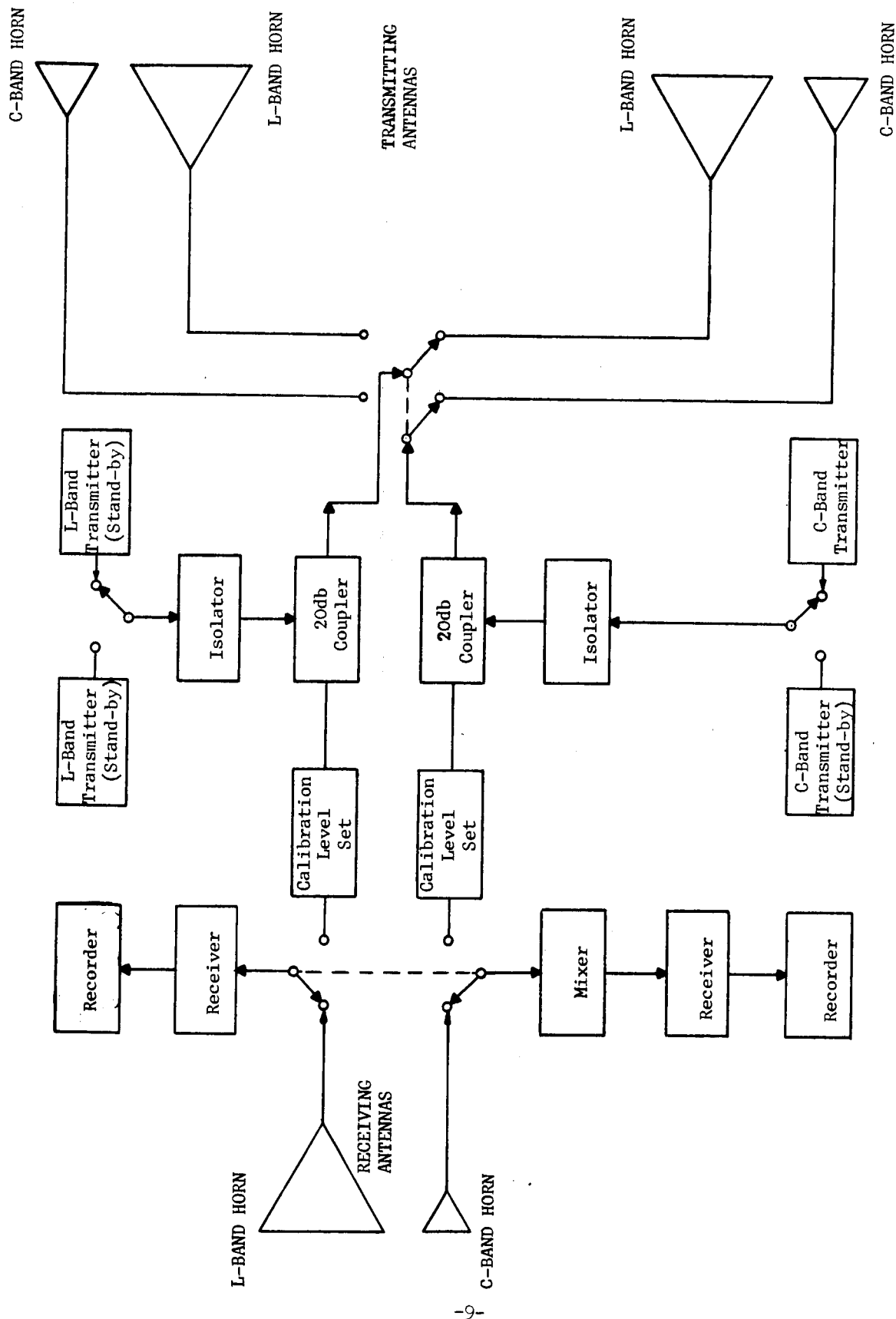


Figure 7 Measurement System Block Diagram

flat plate and its mount is shown in Figure 8.

Immediately prior to the commencement of the reflectivity tests on the balloon, a complete series of flat plate calibration patterns were made. The receiving horns were aligned in the direction of the flat plate, with the receiver cart adjacent to the left transmitter horns. All horns were at vertical polarization. The sources were connected to the left transmitting horns, the flat plate rotated, and reflectivity patterns recorded. The transmitters were then connected to the receivers through attenuators which were adjusted so that the receiver pens coincided with the flat plate maxima. Straight line patterns using these attenuator settings were run. The right transmitters were then connected, new flat plate patterns recorded, and their maxima compared to the straight line pattern. The attenuator settings were then readjusted so as to lie midway between the two flat plate maxima. These adjustments were maintained throughout the test sequence, and used to calibrate all the balloon reflectivity data. At the conclusion of the test, the stability of the sources were tested against flat plate runs. There was no observed change in the calibration level. A typical calibration pattern is shown in Figure 9.

#### MEASUREMENT PROCEDURE

Reflectivity data was obtained on the balloon in the following way. Several hours prior to the beginning of the test, the transmitters were turned on and allowed to warm-up and stabilize. At this time all systems were connected and the horns were aligned on the balloon. The receiver cart was located adjacent to the right transmitters as seen from the console control center.

Upon notification by the NASA Test Director that the balloon had reached a given internal pressure level, the cart was moved to the left and simultaneous recordings of the C-Band and L-Band return signal levels were made as a function of cart position. When the cart reached its left most position, a switch was thrown disconnecting the right transmitters and connecting the left transmitters. The receiver cart was then run back to the right. The return signal levels



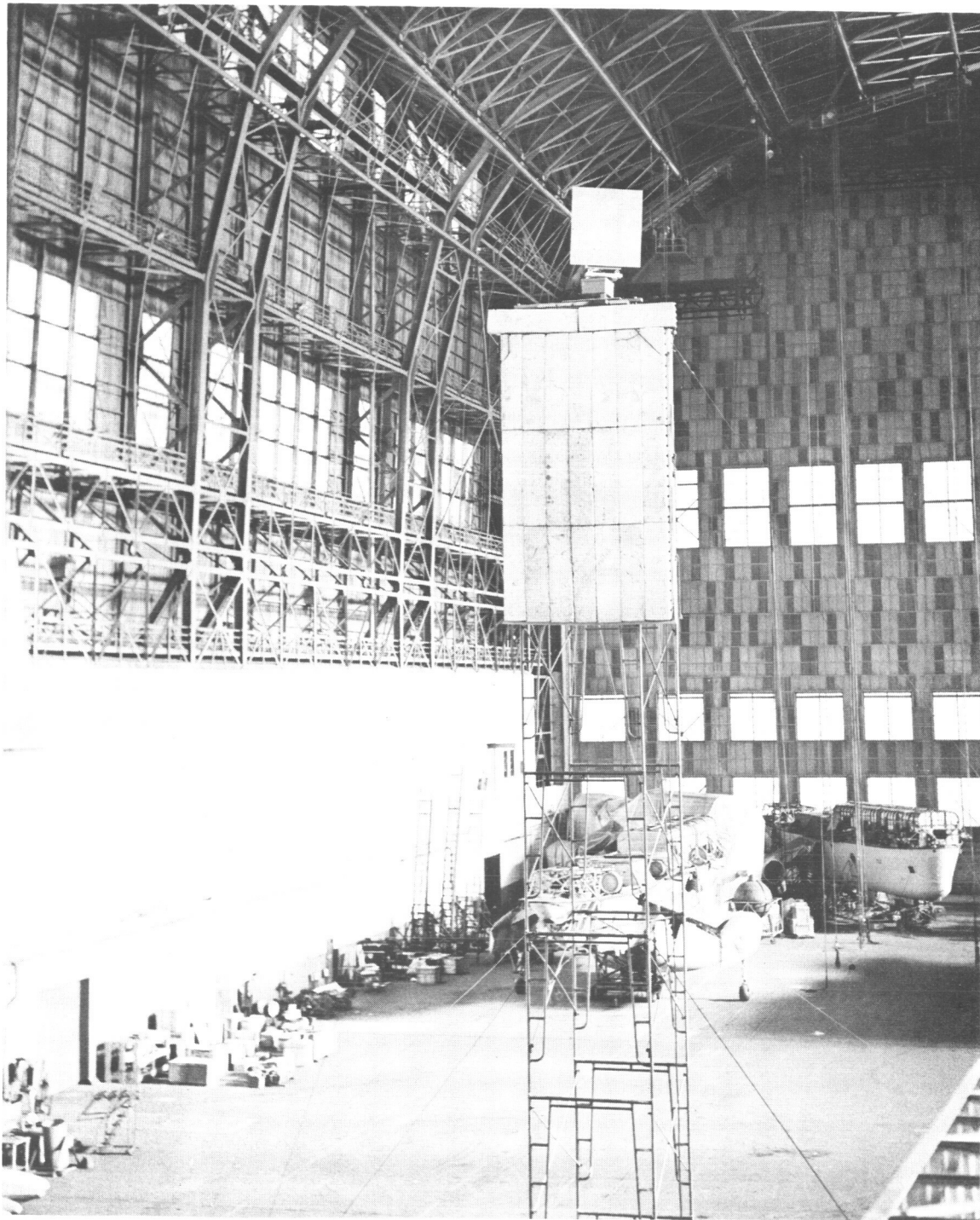


Figure 8

Pattern No.: 5002-3 Date: 12-18-63  
 Project: 36  
 Engineers: HB and FB

REMARKS:

L-Band Calibration Pattern  
 Frequency: 1.70 KMC  
 Polarization: Vertical  
 Transmitter Position: Right  
 $\theta = 25.4 \text{ dB} > \theta_m$

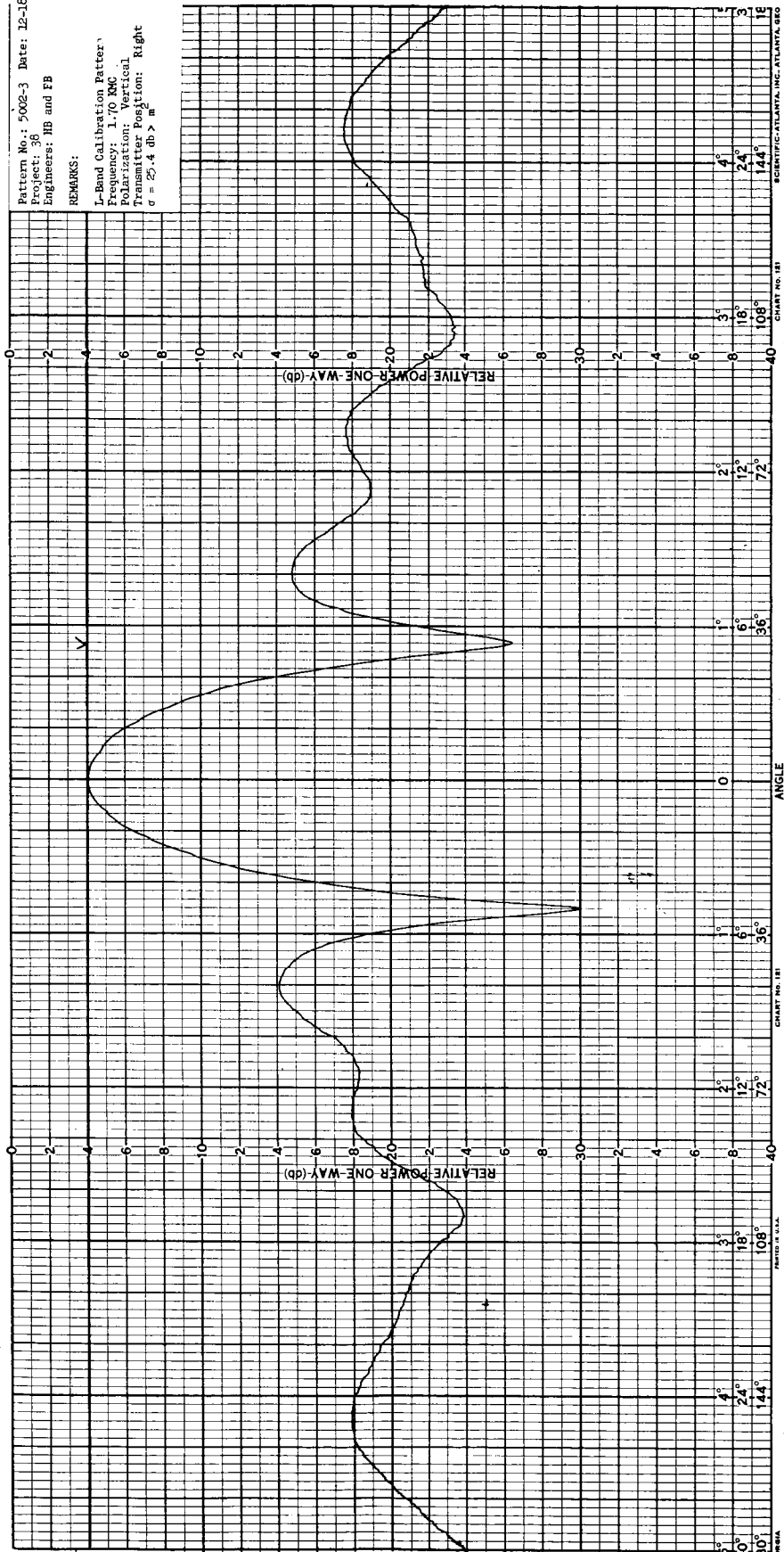


Figure 9

were calibrated using the secondary standard. In this fashion, patterns were obtained at each frequency. For simplicity, the data was labeled either TRANSMIT RIGHT or TRANSMIT LEFT. The data which was obtained is summarized in Table I.

For either transmit position, the bistatic angle increased from  $0^{\circ}$  to  $30^{\circ}$ . The "specular" angle, defined as the bisector of the bistatic angle, changed  $15^{\circ}$ . If the specular angle were redefined to be the angular position on the balloon corresponding to the specular ray, letting for convenience, the right most position correspond to  $0^{\circ}$ , then for TRANSMIT RIGHT, the specular angle increased from  $0^{\circ}$  to  $15^{\circ}$ , and for TRANSMIT LEFT, it decreased from  $30^{\circ}$  to  $15^{\circ}$ .

The balloon was constructed of adjacent gores, each subtending an angle of  $180^{\circ}/53 \sim 3.4^{\circ}$ . The sector of the balloon corresponding to  $0^{\circ}$  -  $15^{\circ}$  contained two adjacent reinforced gores. Therefore, the patterns corresponding to TRANSMIT RIGHT represent a specular angle which passed over the reinforced gores, and those corresponding to TRANSMIT LEFT, represent a specular angle which did not pass over the reinforced gores.

#### BACKGROUND LEVELS

The radar cross section of a conducting sphere 135 feet in diameter is  $1,335 \text{ m}^2$ , or  $31.2 \text{ db} > \text{m}^2$ . In order to insure the validity of the measurement data, the background levels must be maintained at least 10 db and preferably 20 db below this nominal value. The background was composed of energy which was reflected from structures other than the balloon. The background levels in the hanger itself were measured prior to the balloon inflation using the same procedure that was used for the balloon measurements. The data was calibrated with the flat plate and the background levels were found to average 15 db below the nominal balloon return at 1.70 Kmc and 30 db below the nominal balloon return at 5.45 Kmc. A typical background pattern at 5.45 Kmc is shown in Figure 10.

In addition, with the balloon in place, the major sources of background reflections were not illuminated. The balloon intercepted  $44^{\circ}$  of the antenna beam, placing the edges at  $\pm 22^{\circ}$ . The previously measured radiation patterns

TABLE I

Test No.	Pattern No.	Run No.	Frequency (Kmc)	Transmitter Position*	Internal Pressure (max) (psi)	Internal Pressure (min) (psi)	Approximate Skin Stress (psi)
1	5004	1	1.70	Right	.025	.006	1040
	5005	2	1.70	Left	.025	.006	1040
	5006	3	5.45	Right	.025	.006	1040
	5007	4	5.45	Left	.025	.006	1040
2	5008	1	1.70	Right	.06		2400
	5009	2	1.70	Left	.06	None	2400
	5010	3	5.45	Right	.06	Given	2400
	5011	4	5.45	Left	.06		2400
3	5012	1	1.70	Right	.084	.054	3360
	5013	2	1.70	Left	.084	.054	3360
	5014	3	5.45	Right	.084	.054	3360
	5015	4	5.45	Left	.084	.054	3360
4	5016	1	1.70	Right	.024		960
	5017	2	1.70	Left	.024	None	960
	5018	3	5.45	Right	.024	Given	960
	5019	4	5.45	Left	.024		960
5	5020	1	1.70	Right	.06	.058	2400
	5021	2	1.70	Left	.06	.058	2400
	5022	3	5.45	Right	.06	.058	2400
	5023	4	5.45	Left	.06	.058	2400
6	5024	1	1.70	Right	.084	.080	3200
	5025	2	1.70	Left	.084	.080	3200
	5026	3	5.45	Right	.084	.080	3200
	5027	4	5.45	Left	.084	.080	3200
7	5028	1	1.70	Right	.132	.134	5200
	5029	2	1.70	Left	.132	.134	5200
	5030	3	5.45	Right	.132	.134	5200
	5031	4	5.45	Left	.132	.134	5200

\* See explanation, Page 13

Test No.	Pattern No.	Run No.	Frequency (Kmc)	Transmitter Position*	Internal Pressure (max) (psi)	Internal Pressure (min) (psi)	Approximate Skin Stress (psi)
8	5032	1	1.70	Right	.178		7120
	5033	2	1.70	Left	.178	None	7120
	5034	3	5.45	Right	.178	Given	7120
	5035	4	5.45	Left	.178		7120
9	5036	1	1.70	Right	.014	.010	560
	5037	2	1.70	Left	.014	.010	560
	5038	3	5.45	Right	.014	.010	560
	5039	4	5.45	Left	.014	.010	560
10	5040	1	1.70	Right	.132		5280
	5041	2	1.70	Left	.132	None	5280
	5042	3	5.45	Right	.132	Given	5280
	5043	4	5.45	Left	.132		5280
11	5044	1	1.70	Right	.182	.180	7281
	5045	2	1.70	Left	.182	.180	7281
	5046	3	5.45	Right	.182	.180	7281
	5047	4	5.45	Left	.182	.180	7281
12	5048	1	1.70	Right	.224	.222	8880
	5049	2	1.70	Left	.224	.222	8880
	5050	3	5.45	Right	.244	.222	8880
	5051	4	5.45	Left	.244	.222	8880
13	5052	1	1.70	Right	.300		12,000
	5053	2	1.70	Left	.300	None	12,000
	5054	3	5.45	Right	.300	Given	12,000
	5055	4	5.45	Left	.300		12,000
14	5056	1	1.70	Right	.366	.352	14,640
	5057	2	1.70	Left	.366	.352	14,640
	5058	3	5.45	Right	.366	.352	14,640
	5059	4	5.45	Left	.366	.352	14,640

\* See explanation, Page 13

Test No.	Pattern No.	Run No.	Frequency (Kmc)	Transmitter Position*	Internal Pressure (max) (psi)	Internal Pressure (min) (psi)	Approximate Skin Stress (psi)
15	5060	1	1.70	Right	.406	.398	16,240
	5061	2	1.70	Left	.406	.398	16,240
	5062	3	5.45	Right	.406	.398	16,240
	5063	4	5.45	Left	.406	.398	16,240
16	5064	1	1.70	Right	.444	.436	17,760
	5065	2	1.70	Left	.444	.436	17,760
	5066	3	5.45	Right	.444	.436	17,760
	5067	4	5.45	Left	.444	.436	17,760
17	5068	1	1.70	Right	.496	.468	18,960
	5069	2	1.70	Left	.496	.468	18,960
	5070	3	5.45	Right	.496	.468	18,960
	5071	4	5.45	Left	.496	.468	18,960
18	5072	1	1.70	Right	.504	.500	20,000
	5073	2	1.70	Left	.504	.500	20,000
	5074	3	5.45	Right	.504	.500	20,000
	5075	4	5.45	Left	.504	.500	20,000
19	5076	1	1.70	Right	.538	.534	21,530
	5077	2	1.70	Left	.538	.534	21,530
	5078	3	5.45	Right	.538	.534	21,530
	5079	4	5.45	Left	.538	.534	21,530
20	5080	1	1.70	Right	.560		22,400
	5081	2	1.70	Left	.560	None	22,400
	5082	3	5.45	Right	.560	Given	22,400
	5083	4	5.45	Left	.560		22,400

\* See explanation, Page 13

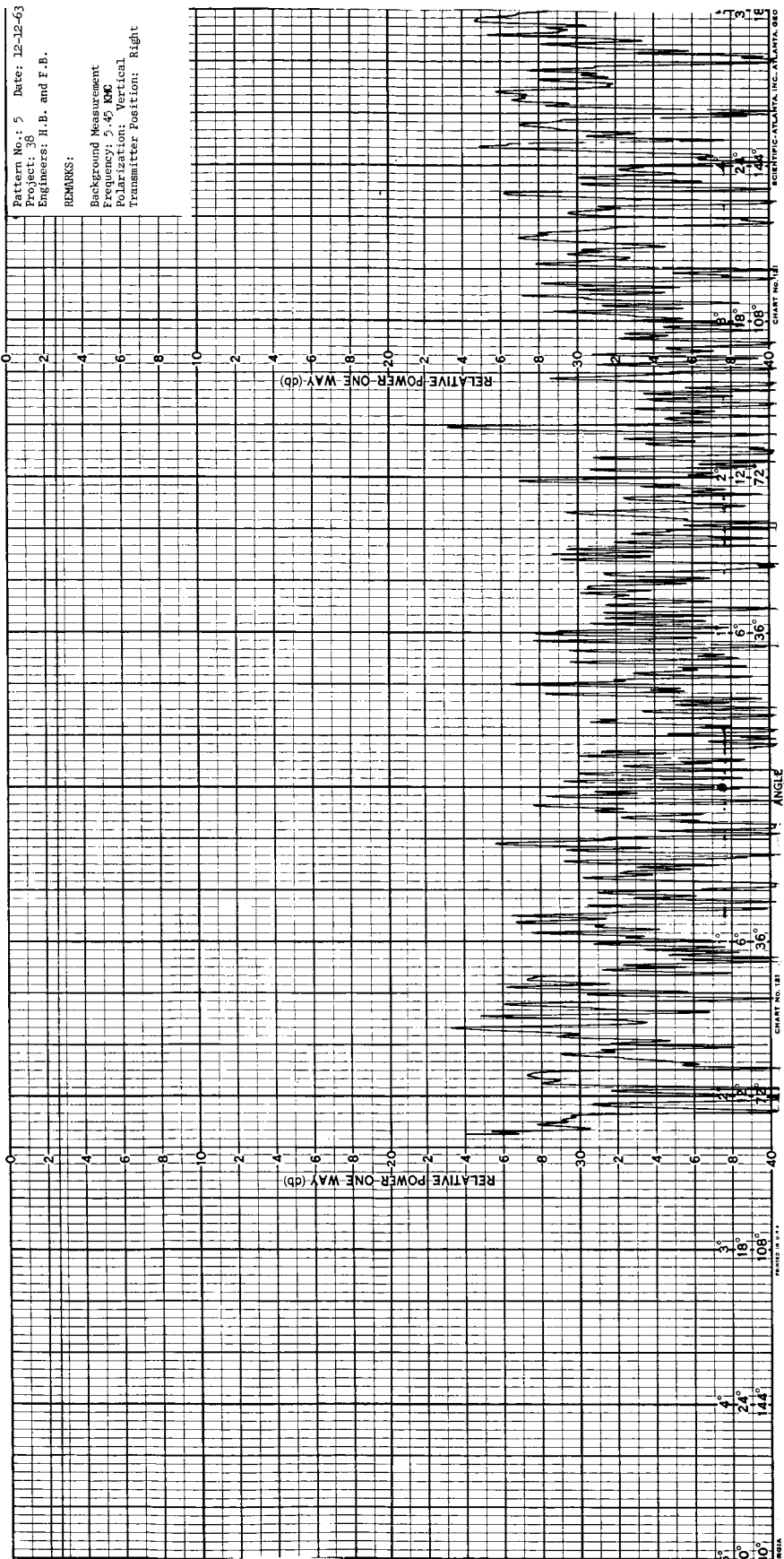


Figure 10

of the horn antennas show that the power gain is approximately 11 db below the pattern maximum. A typical antenna pattern is shown in Figure 11. A more serious background effect, caused by direct cross-coupling between the transmitting and receiving antennas, was experienced during the SIT - July. However, this effect was minimized by placing dielectric absorber sheets next to the transmitting antennas thus shielding them from the receiving antennas. The result was to eliminate completely the apparent coupling at both L-Band and C-Band.

COMPARISON OF THE SIT DEC-1963 WITH THE SIT JUNE-JULY-1963.

The measurements described in this report were made as part of a continuing program for the evaluation of the radar reflectivity properties of the ECHO-II balloon. As a previous part of this program, radar reflection data were obtained on three other balloons during June and July 1963, and are reported in the Phase B Final Report<sup>1</sup>. The December tests differed from the June - July tests in both the reflection measurement and inflation procedures.

The measurement procedure differed in several aspects. During the July tests, the primary emphasis was placed on the quantity of data to be obtained at a specific pressure level rather than the speed of the measurement sequence. Accordingly, the number of measurements at a given pressure level was much greater than was required in the December tests. The July test requirements were originally for both horizontal and vertical polarizations (and, in some cases, cross polarization), and four frequencies. For the December test the primary emphasis was shifted to accelerated pressure testing. Accordingly, the measurement requirements were reduced to one polarization and two frequencies. Two receivers and two recorders were employed so that simultaneous data could be taken at both of the required frequencies. The antenna mounts facilitated the antenna alignment and the speed of the receiver cart was

---

<sup>1</sup> Conductron Corporation Report No. 0038-B-F under Contract No. NAS 5-3232, Prepared for NASA, Communication Research Branch, Greenbelt, Maryland, December 1963, Unclassified.



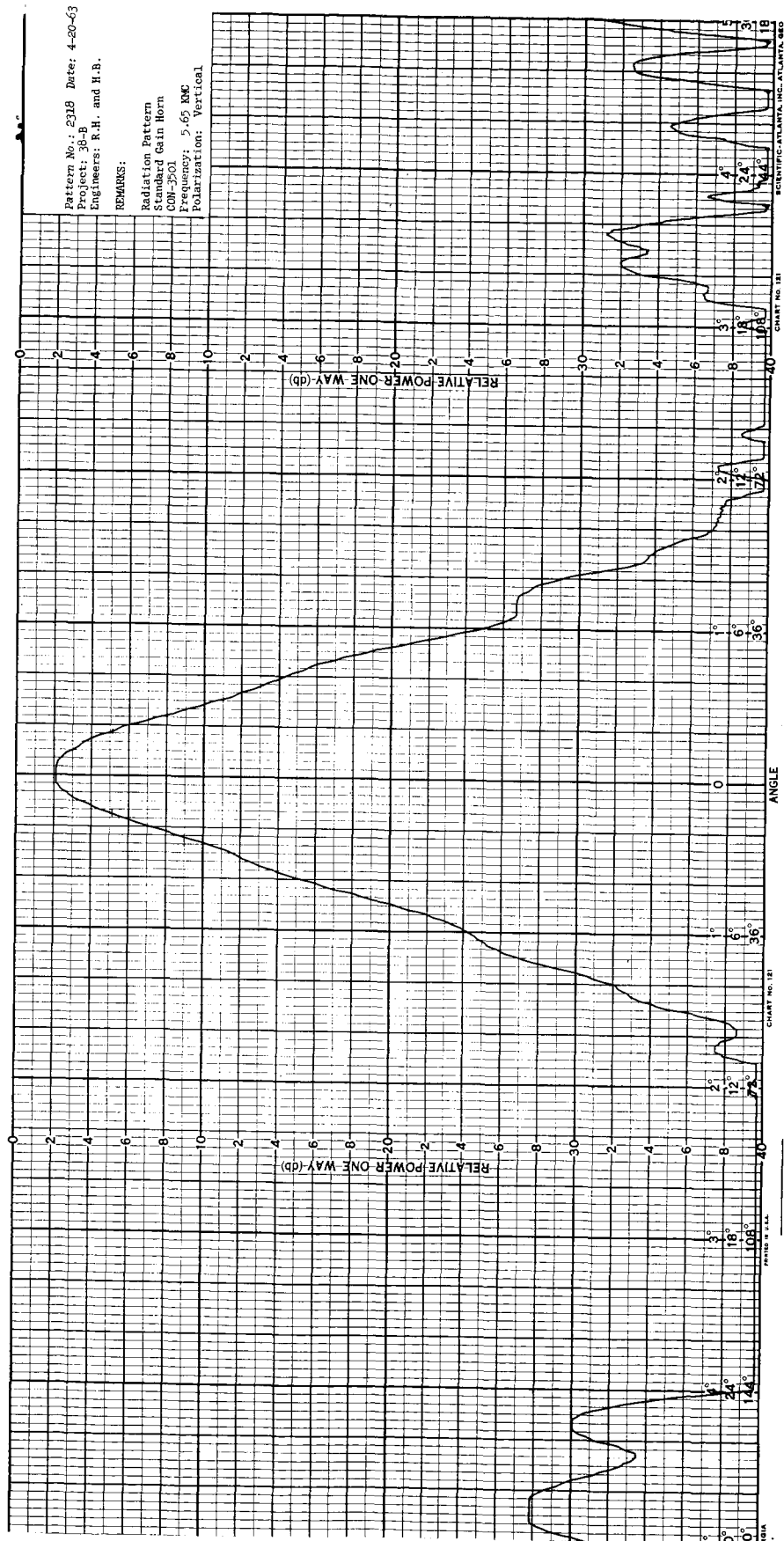


Figure 11

increased to a maximum of approximately 2.5 ft/sec. With these changes, it was possible to obtain the required data at both frequencies for one pressure level in less than 3 minutes.

In the July tests, the procedure was to make a reflection test at some internal pressure level, and then to reduce the pressure to ambient and repeat the test. In the December test, the pressure was reduced to ambient only twice during the entire test, but reflection measurements were made throughout the inflation history. Figure 12 is a graph showing pressure as a function of time over the test period. The times when reflection measurements were made are shown on the graph. It should be noted that the pressure level was constantly fluctuating and the reflection measurements were timed to be made during pressure peaks insofar as was possible. Thus, the data which was obtained during the December tests much more completely described the radar reflectivity of the balloon as a function of internal pressure than was possible with the data obtained during the July tests.

#### DISCUSSION OF DATA

The graphical summary of the data obtained is presented in Figures 13 through 58.

Figures 13 through 32, bearing the legends Test #1 to Test #20, show the L-Band and C-Band radar cross section return from  $0^{\circ}$  to  $30^{\circ}$ . The heavy line on these graphs is the mean cross section of  $2.5^{\circ}$  intervals and the dotted lines indicated the limits of the scintillations taken over these intervals. On each graph for each frequency is listed the average value of the total peak to peak scintillation.

It should be observed that the C-Band average cross section as obtained from these graphs is from 3 to 4 db below the L-Band average cross section. The calibration and measurement procedures have been reviewed and do not appear to offer a suitable explanation for this phenomenon. However, it should be noted that there is a high degree of correlation between the average cross section curves for both L-Band and C-Band at a given pressure level. For example, in Figure 15 the maxima and minima of the average cross section curves

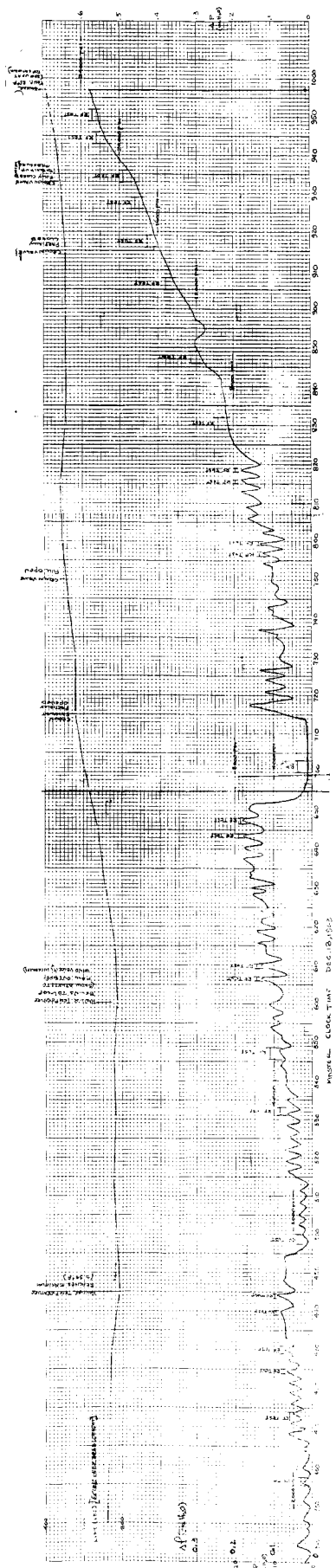
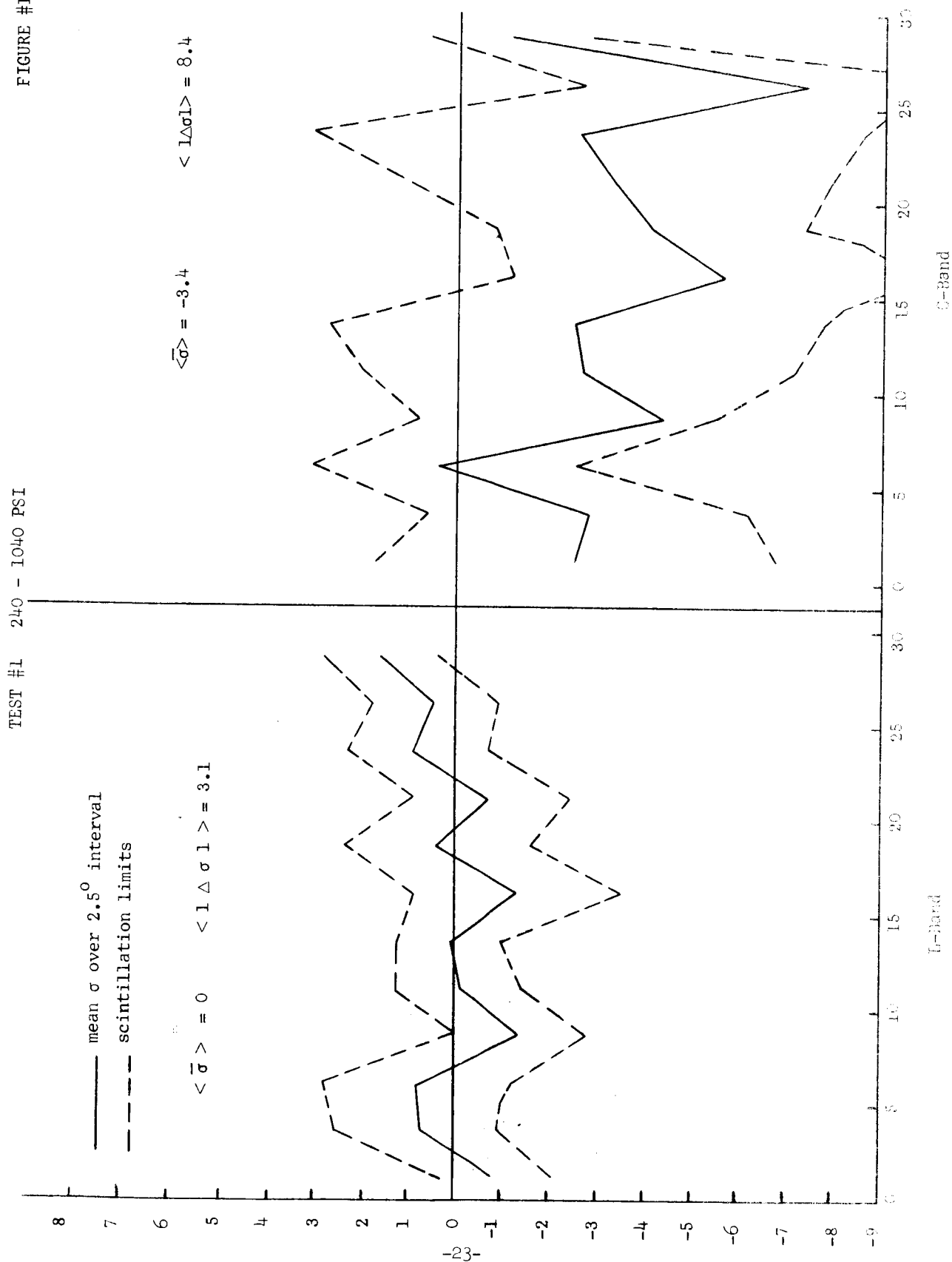


Figure 12

occur at about the same bistatic angles for both the L-Band and C-Band curves. This observation adds support to the assumption that the C-Band data has simply been displaced, and that this displacement has not altered the scintillation history as a function of the internal pressure of the balloon.

Figures 33 through 56 show the average and the limits of the radar cross section data over  $2.5^{\circ}$  intervals as a function of test numbers. Figures 57 and 58 show the history of the average and the limits of the radar cross section data over the full  $30^{\circ}$  interval as a function of test number.

FIGURE #13



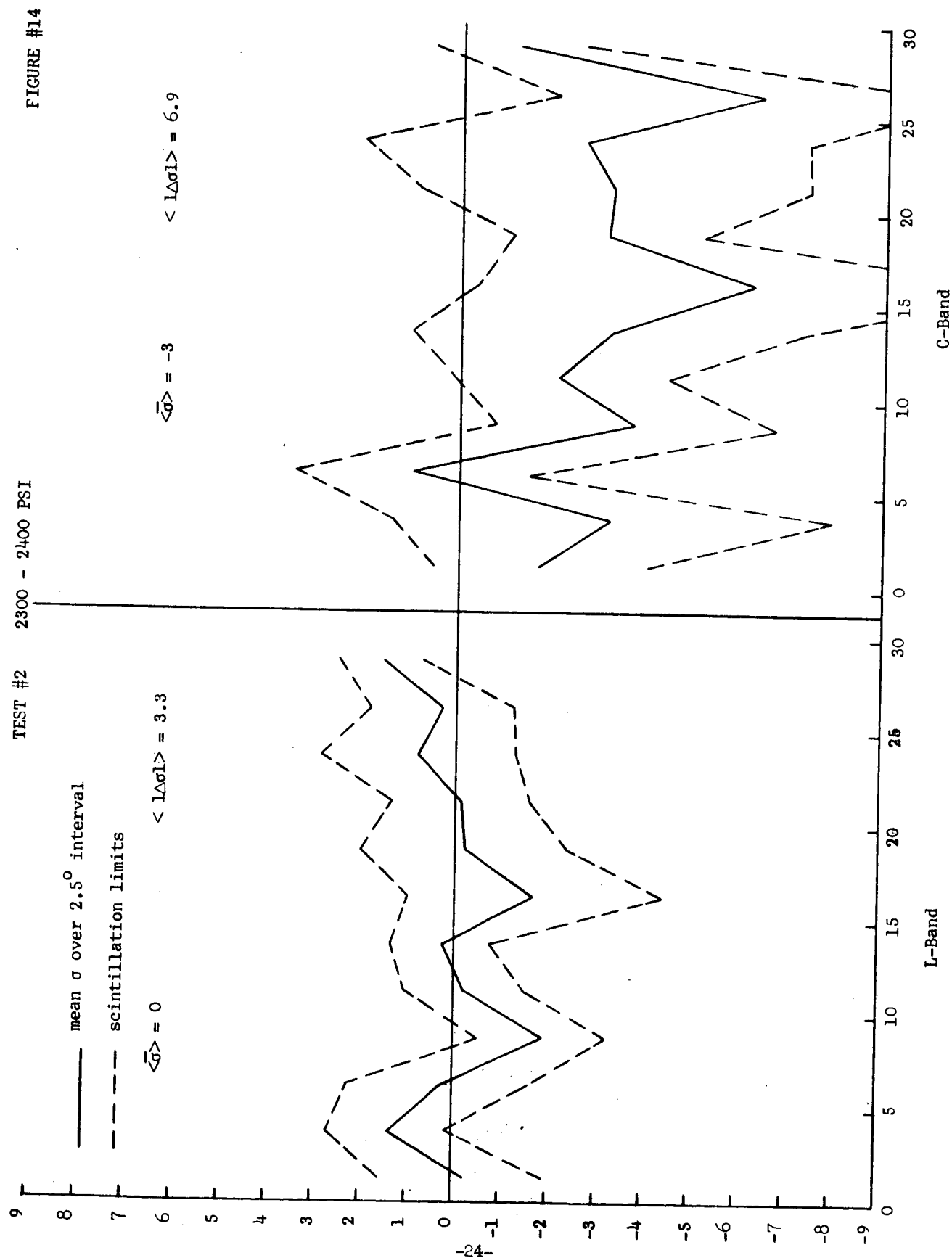


FIGURE #15

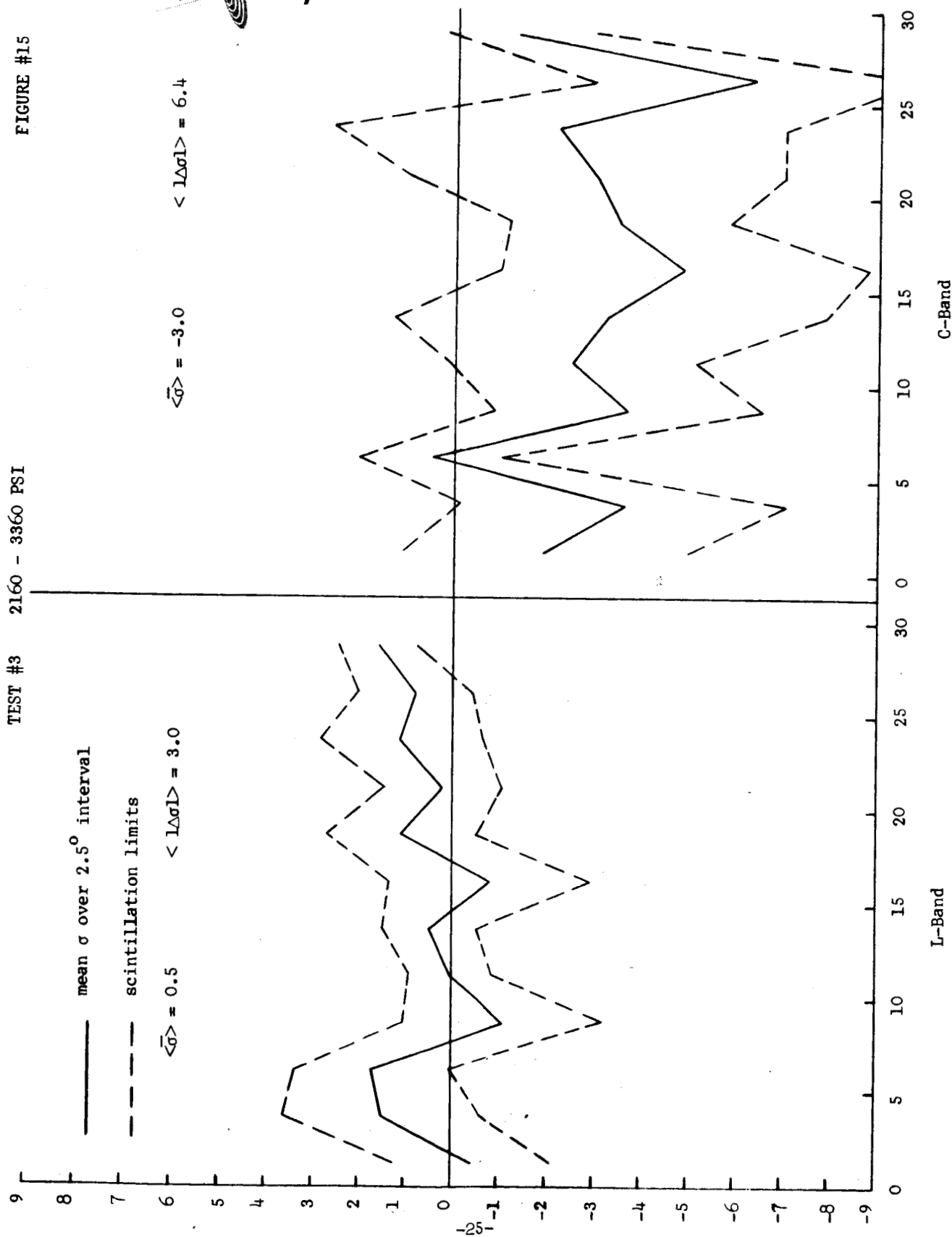


FIGURE #16

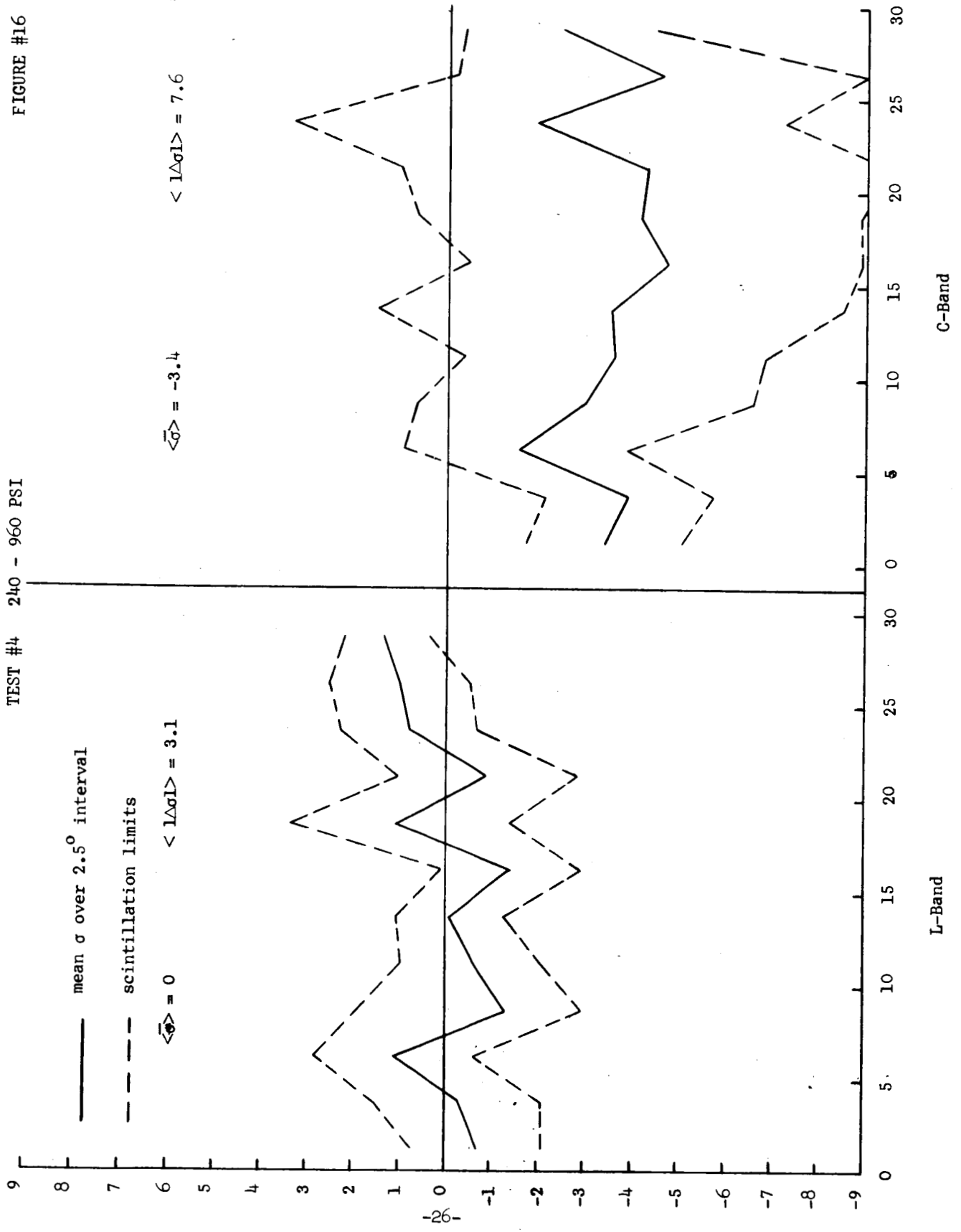




FIGURE #17

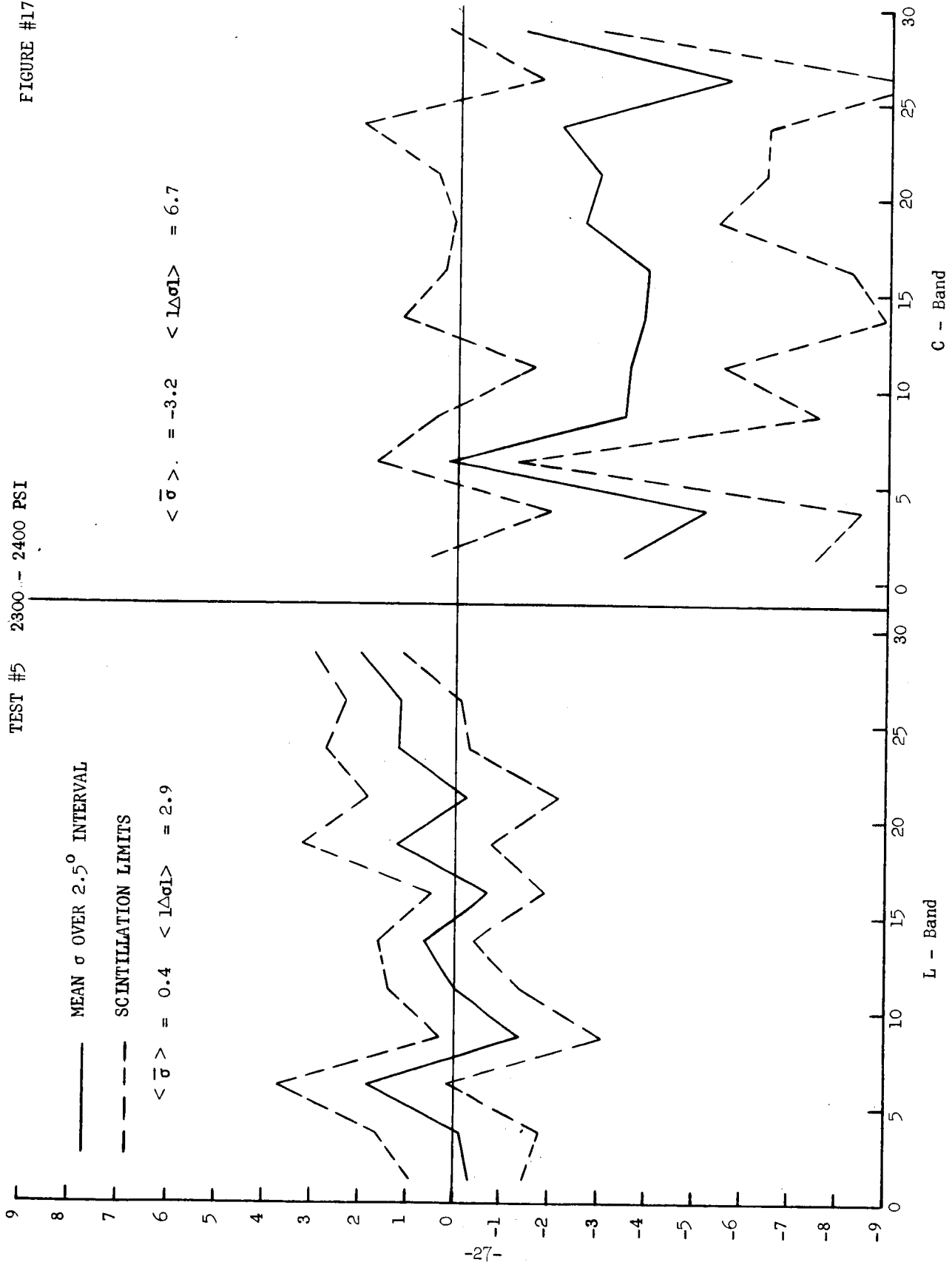


FIGURE #18

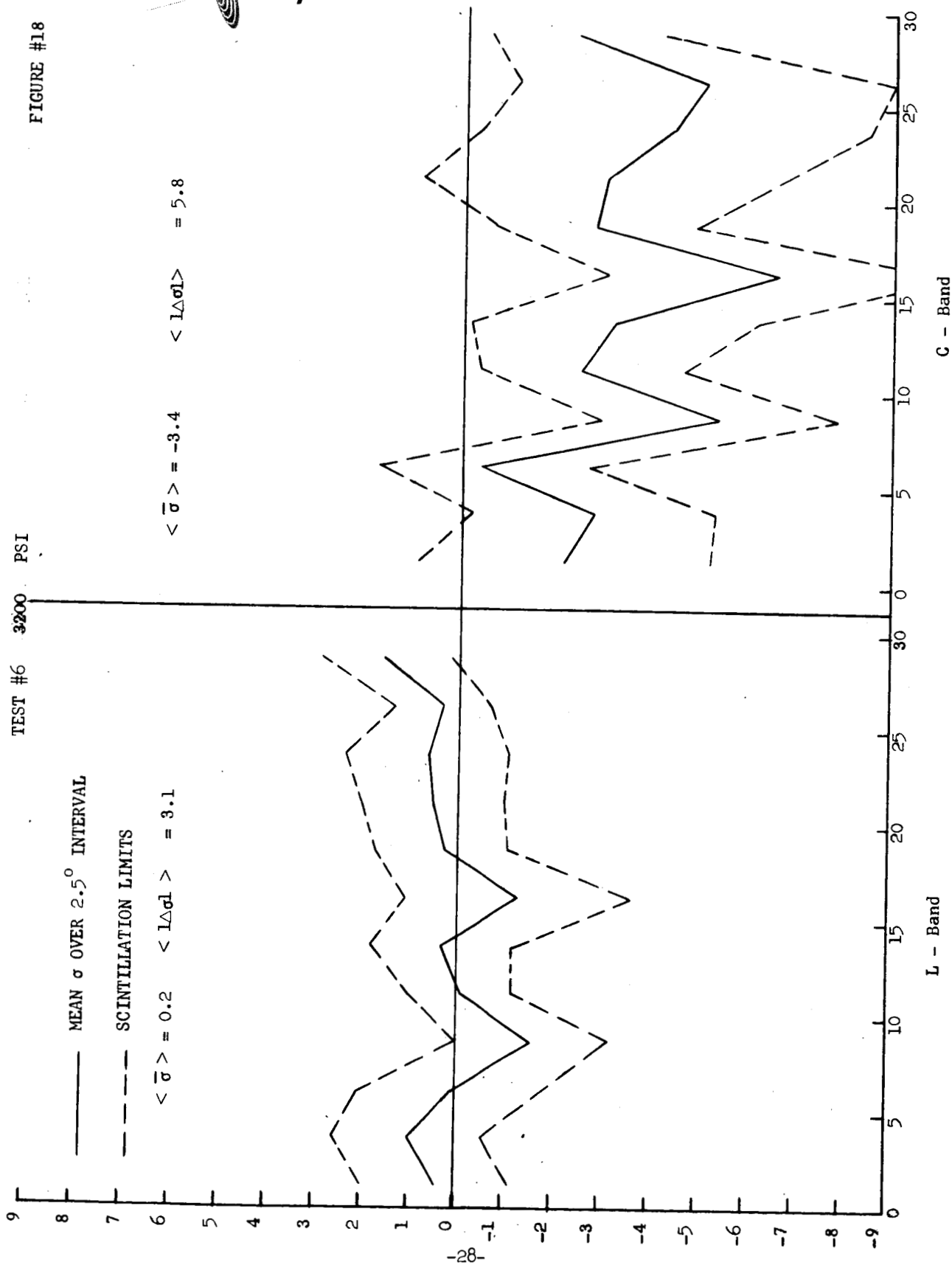


FIGURE #19

TEST #7 4400. - 5200 PSI

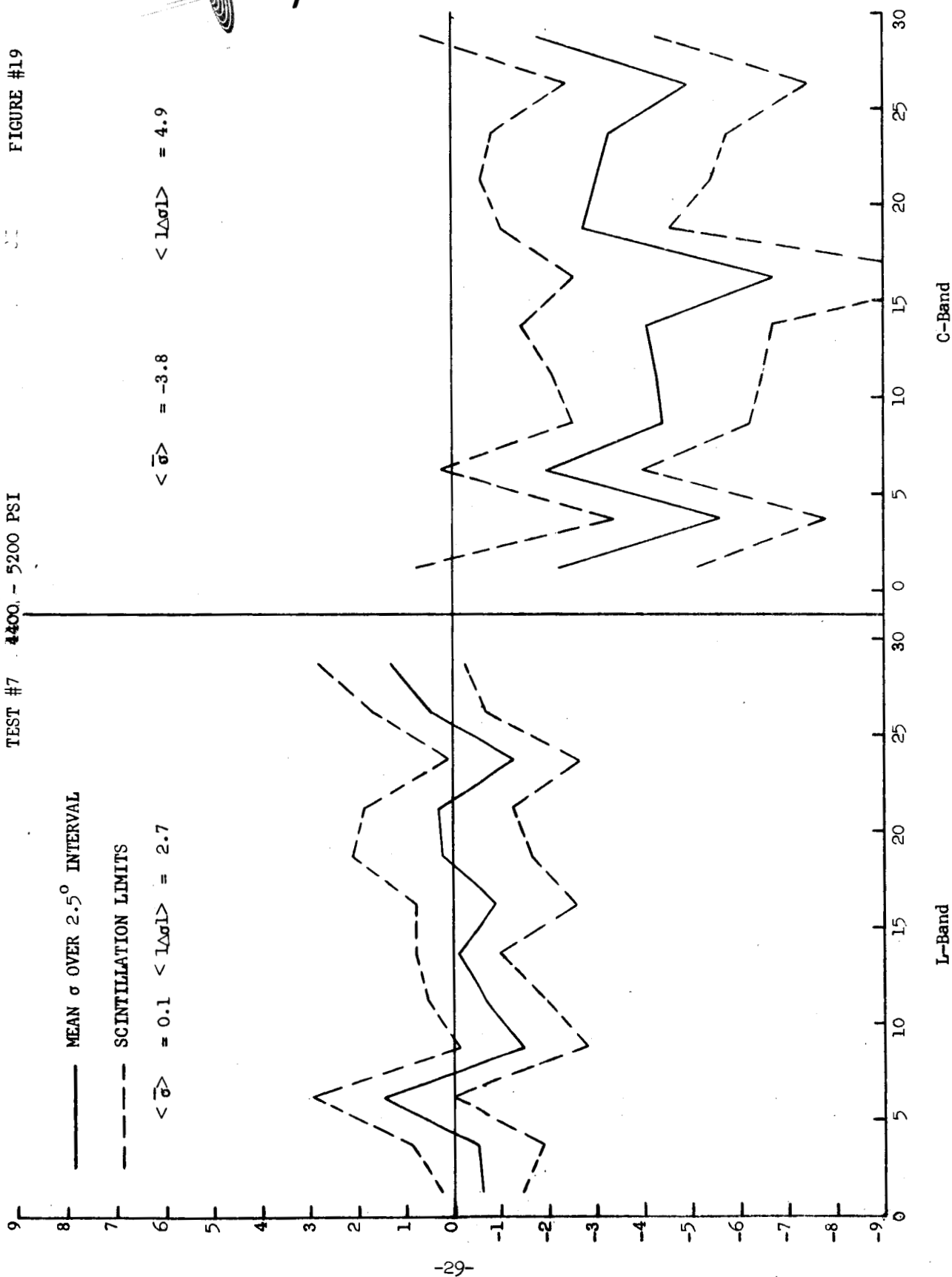


FIGURE #20

TEST #3 7120 PSI

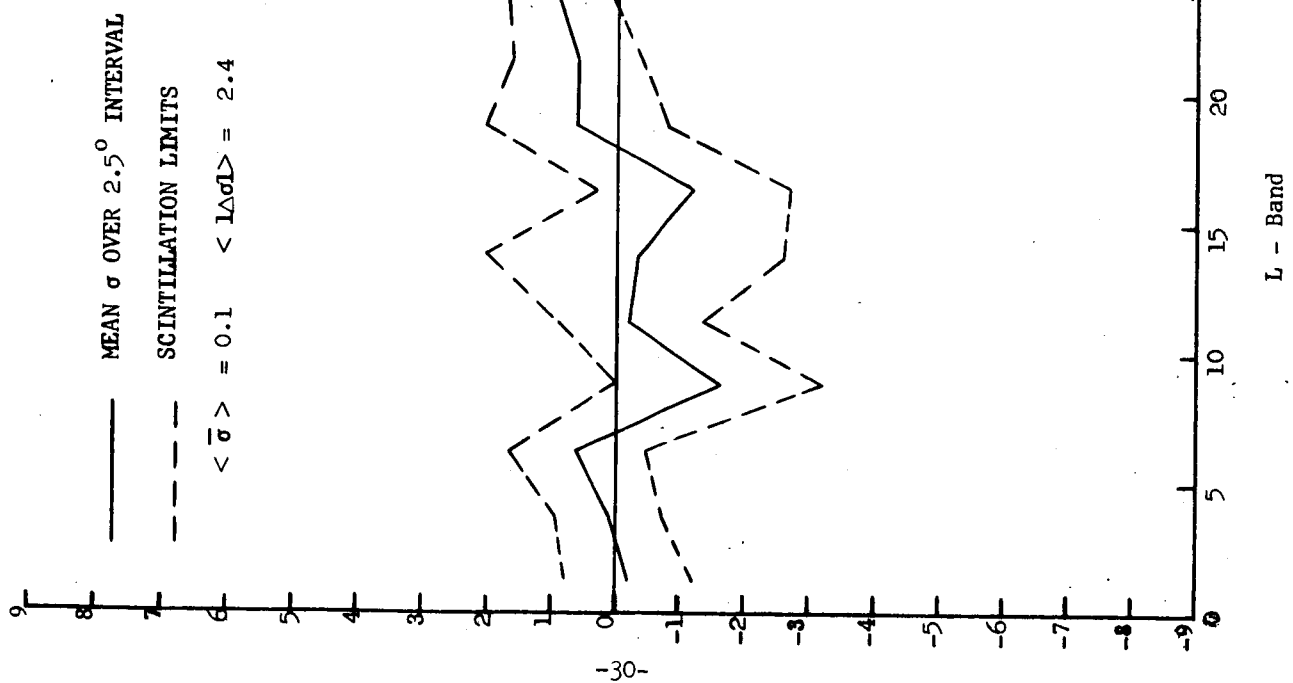


FIGURE #21

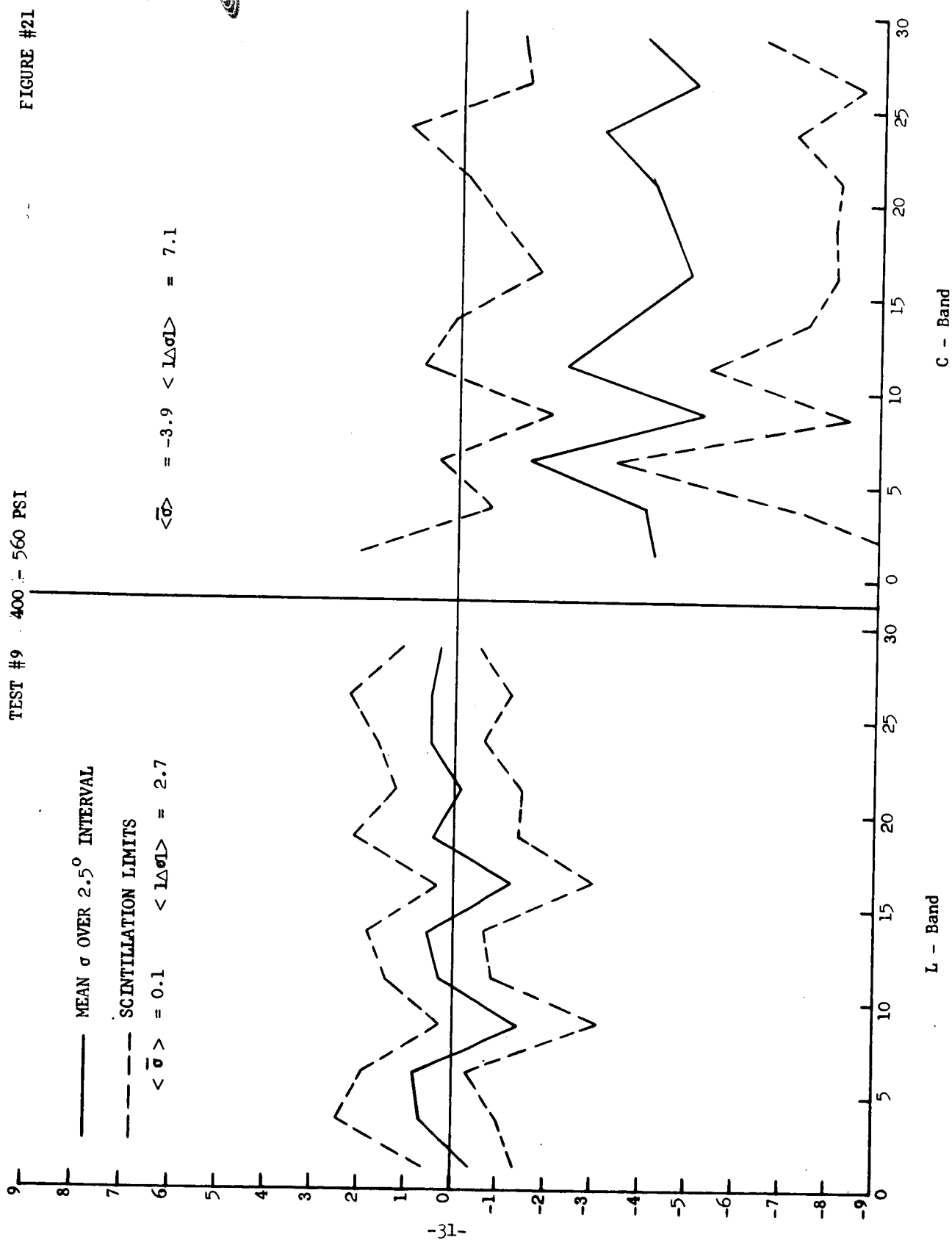


FIGURE #22

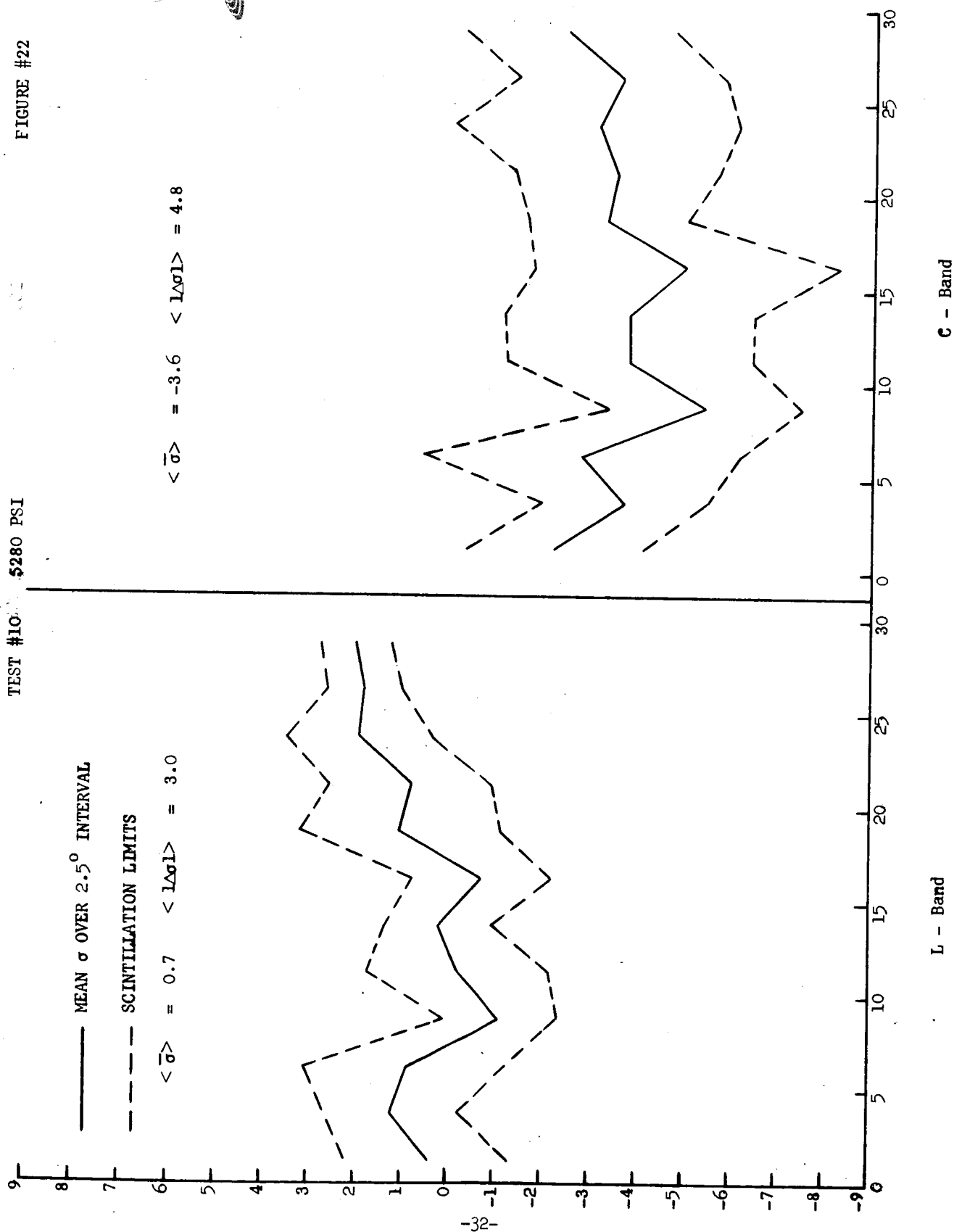


FIGURE # 23

TEST #11 7200 - 7280 PSI

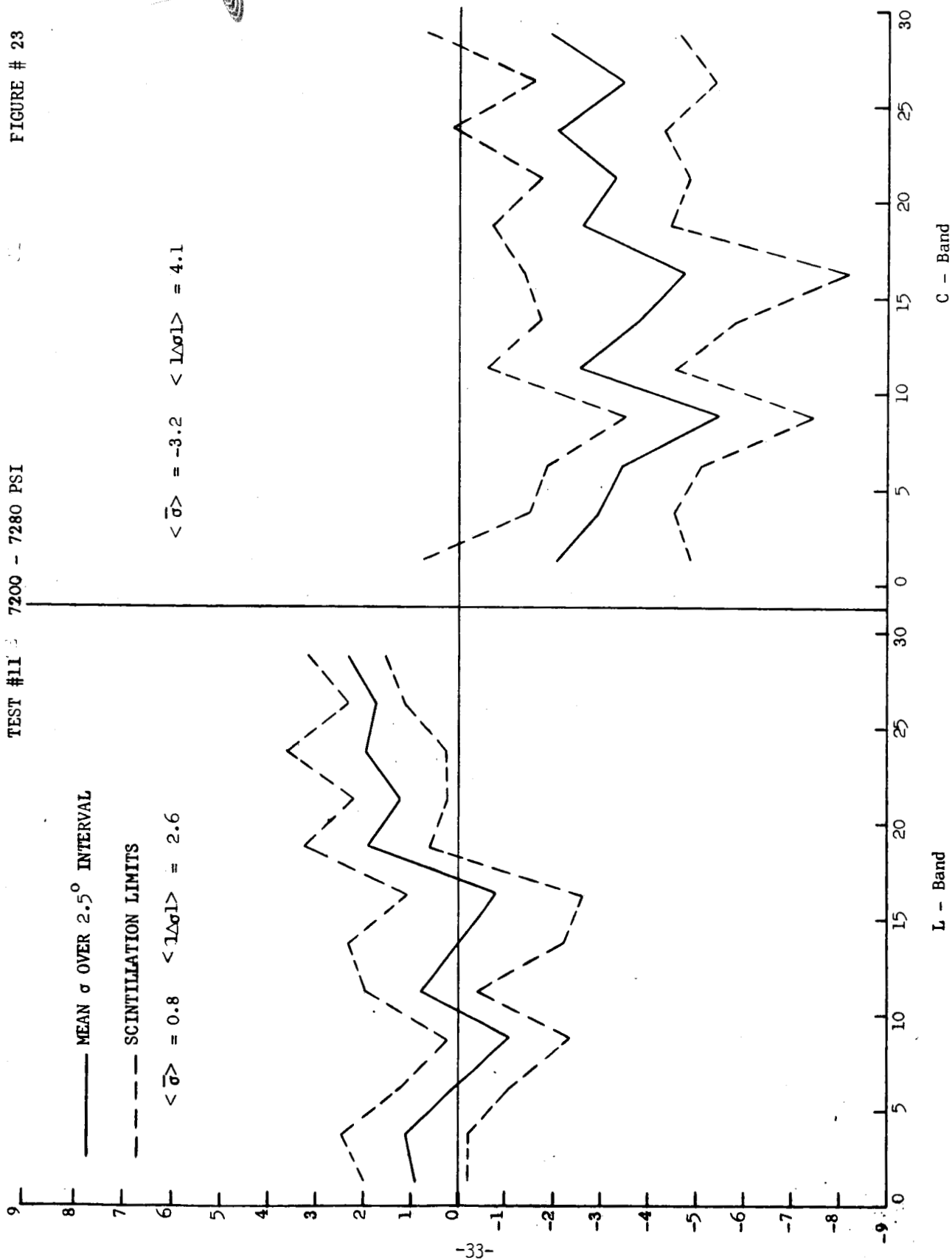


FIGURE #24

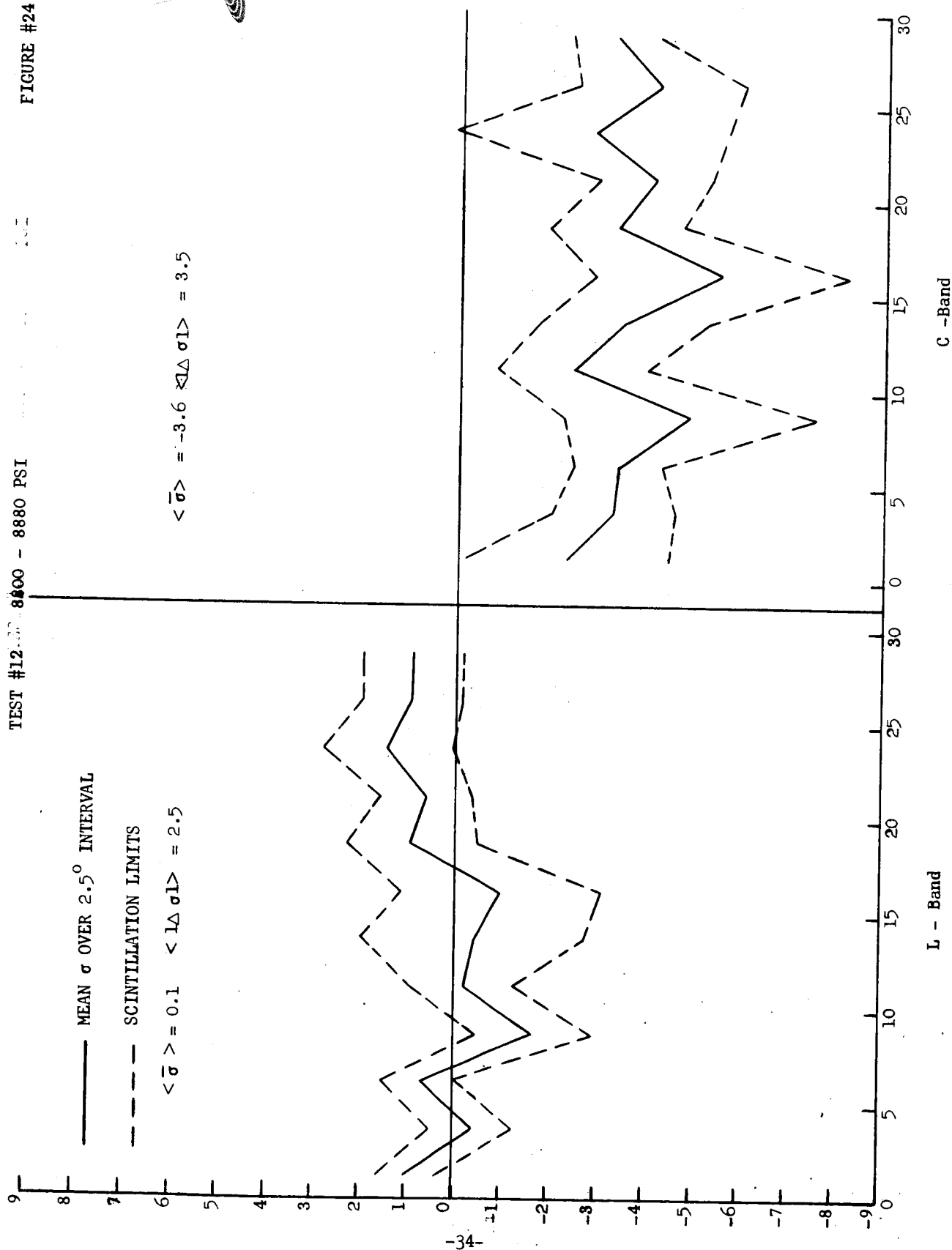




FIGURE #25

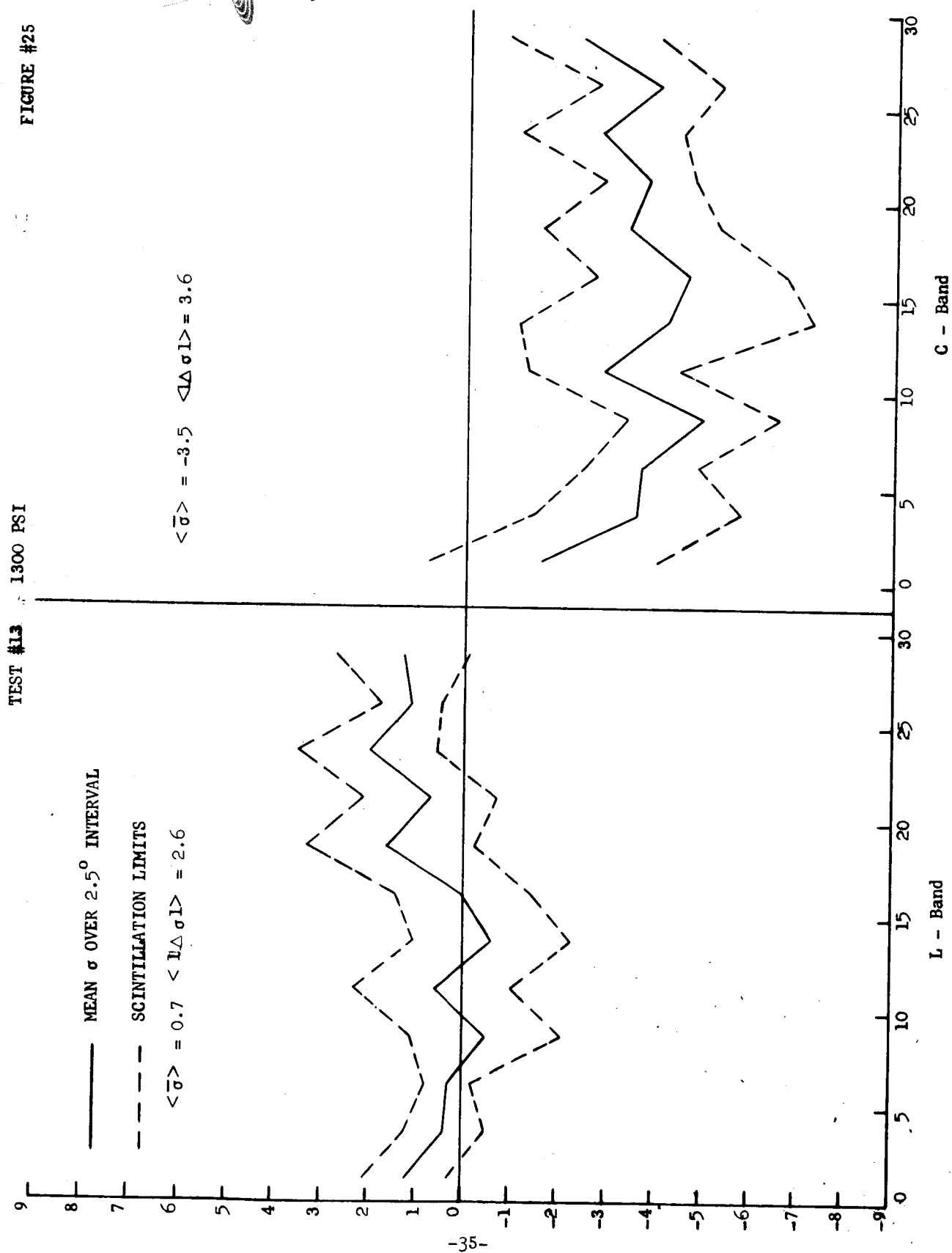


FIGURE #26

TEST #14 14280 - 14640 PSI

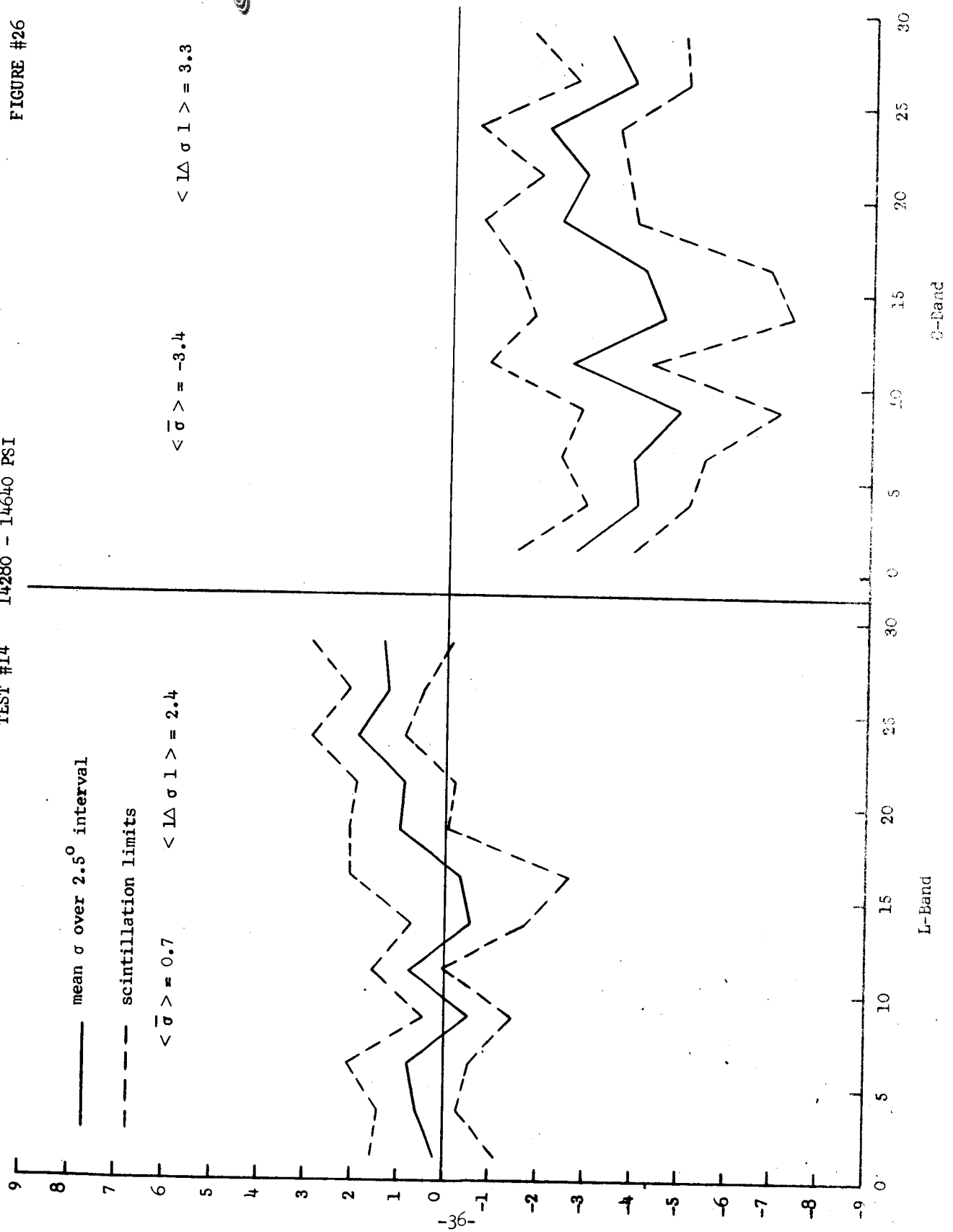


FIGURE #27

TEST #15 15920 - 16240 PSI

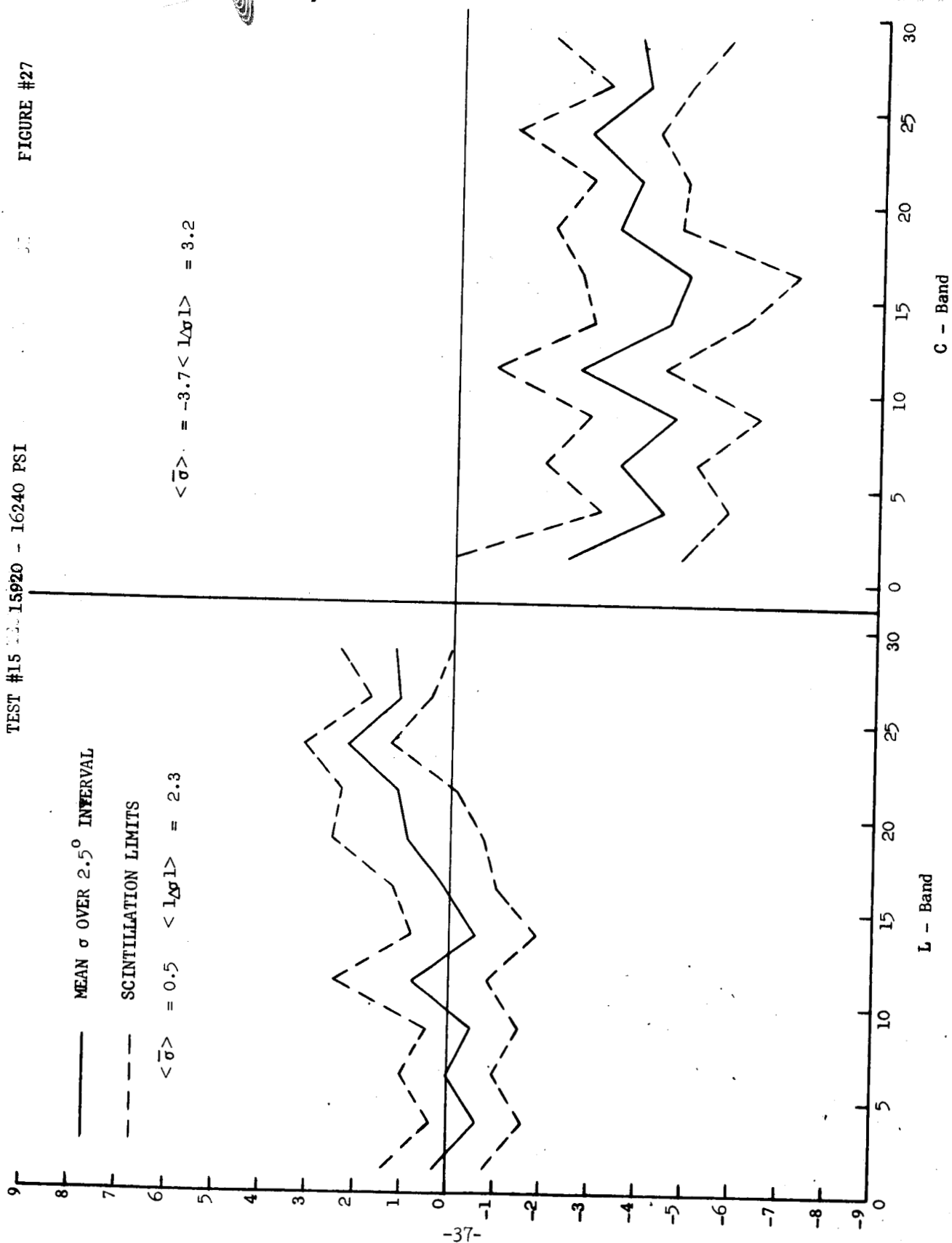


FIGURE #28

TEST #16 17440 - 17760 PSI

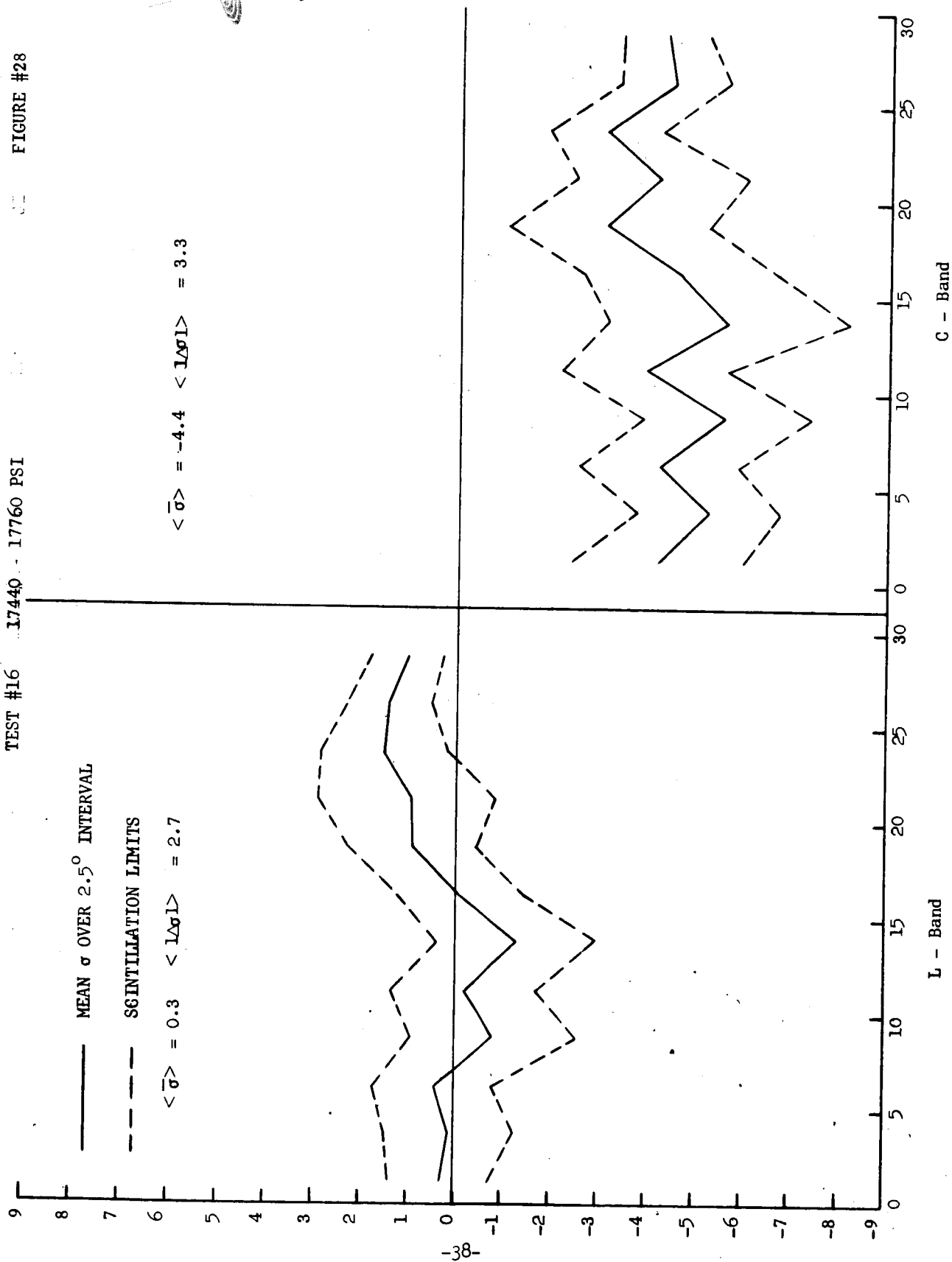


FIGURE #29

TEST #17 18720 - 19840 PSI

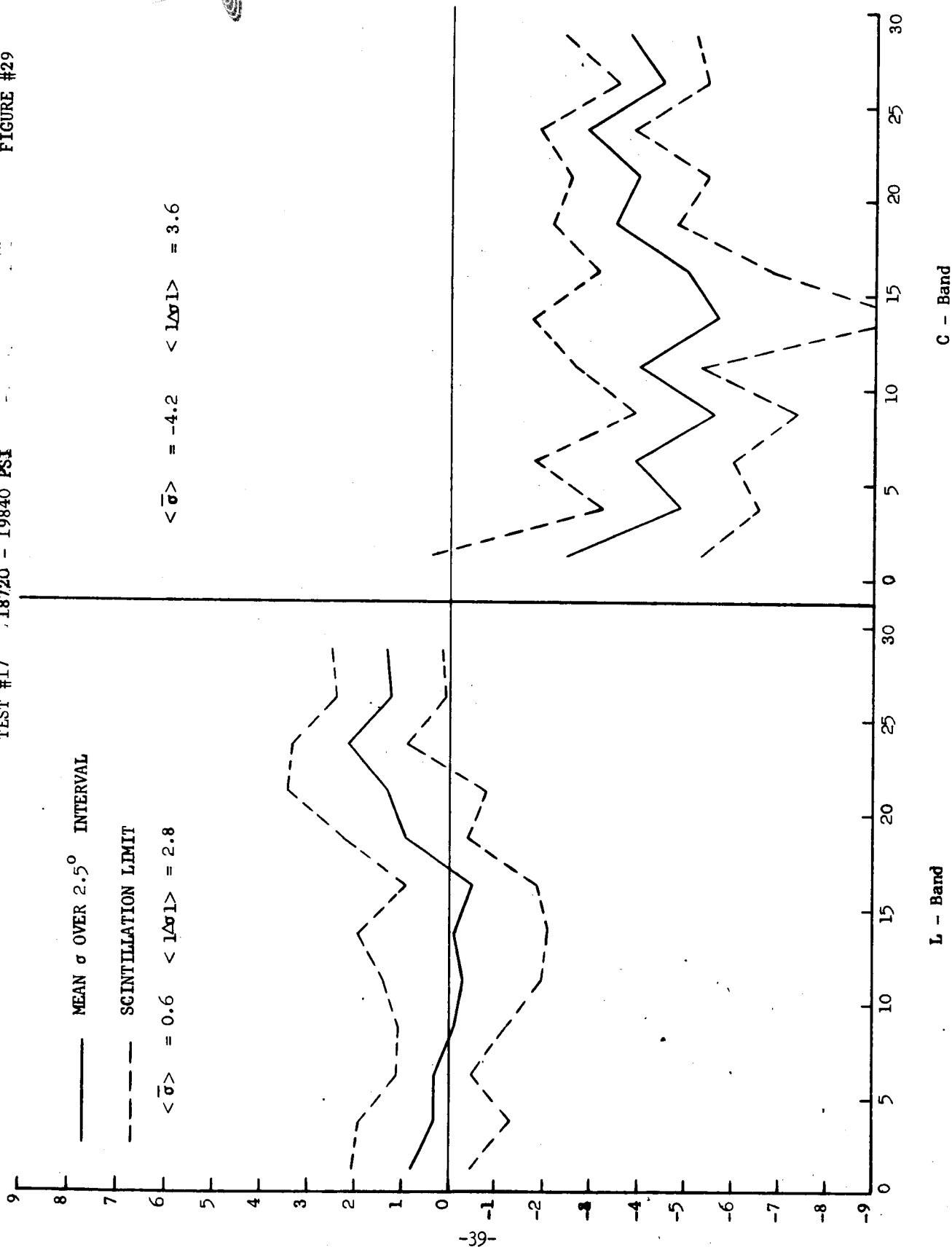


FIGURE #30

101

TEST #18 200000 - 20160 PSI

9  
8  
7  
6  
5  
4  
3  
2  
1  
0  
-1  
-2  
-3  
-4  
-5  
-6  
-7  
-8  
-9

— MEAN  $\sigma$  OVER 2.5° INTERVAL

- - - SCINTILLATION LIMIT

$\langle \bar{\sigma} \rangle > 0.4 \quad \langle \Delta \sigma \rangle > 2.5$

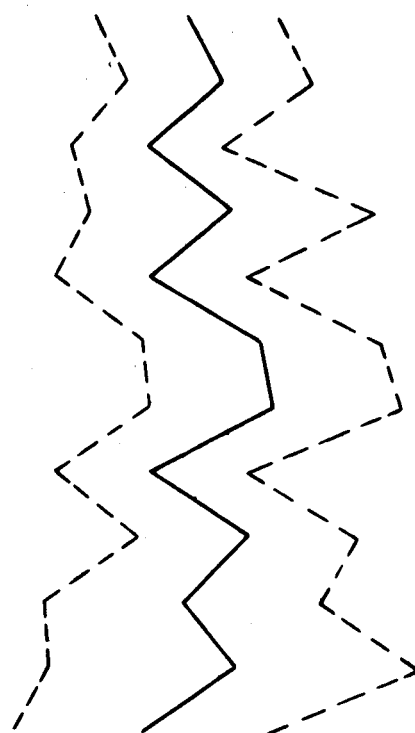
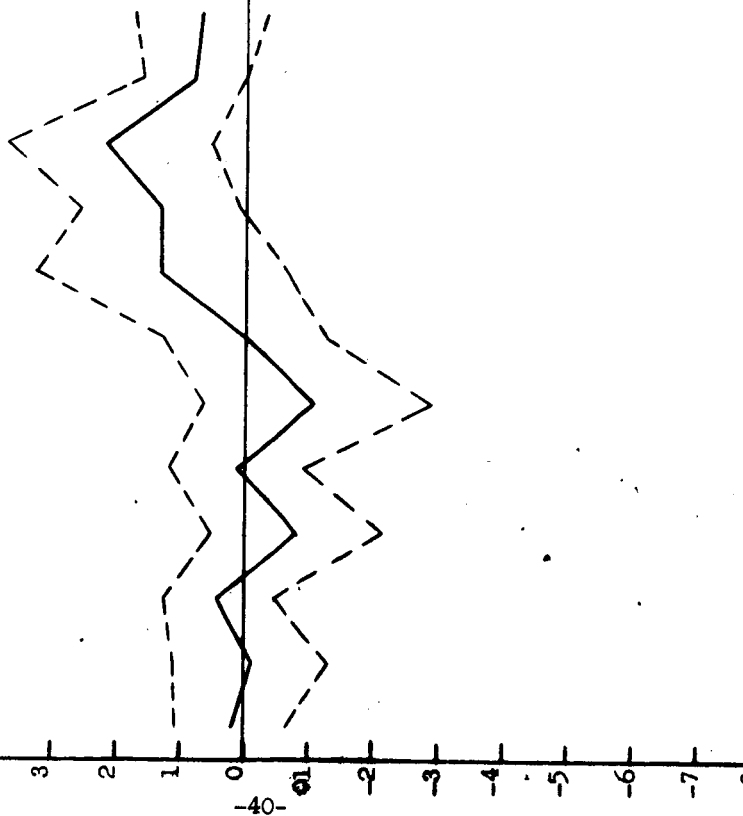
$\langle \bar{\sigma} \rangle < -4.3 \quad \langle \Delta \sigma \rangle > 3.6$

-40-

L - Band

C - Band

0 5 10 15 20 25 30 0 5 10 15 20 25 30



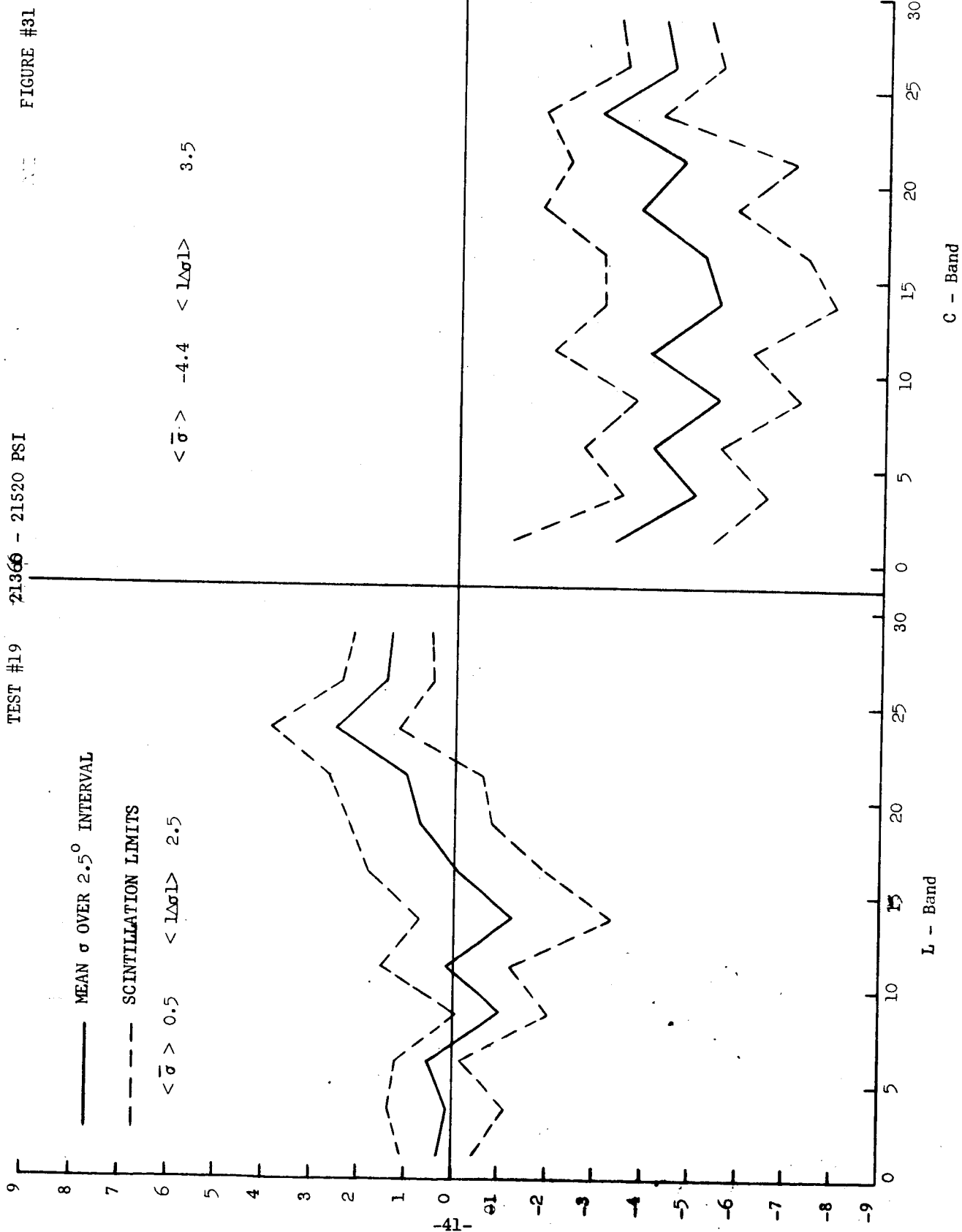


FIGURE #32

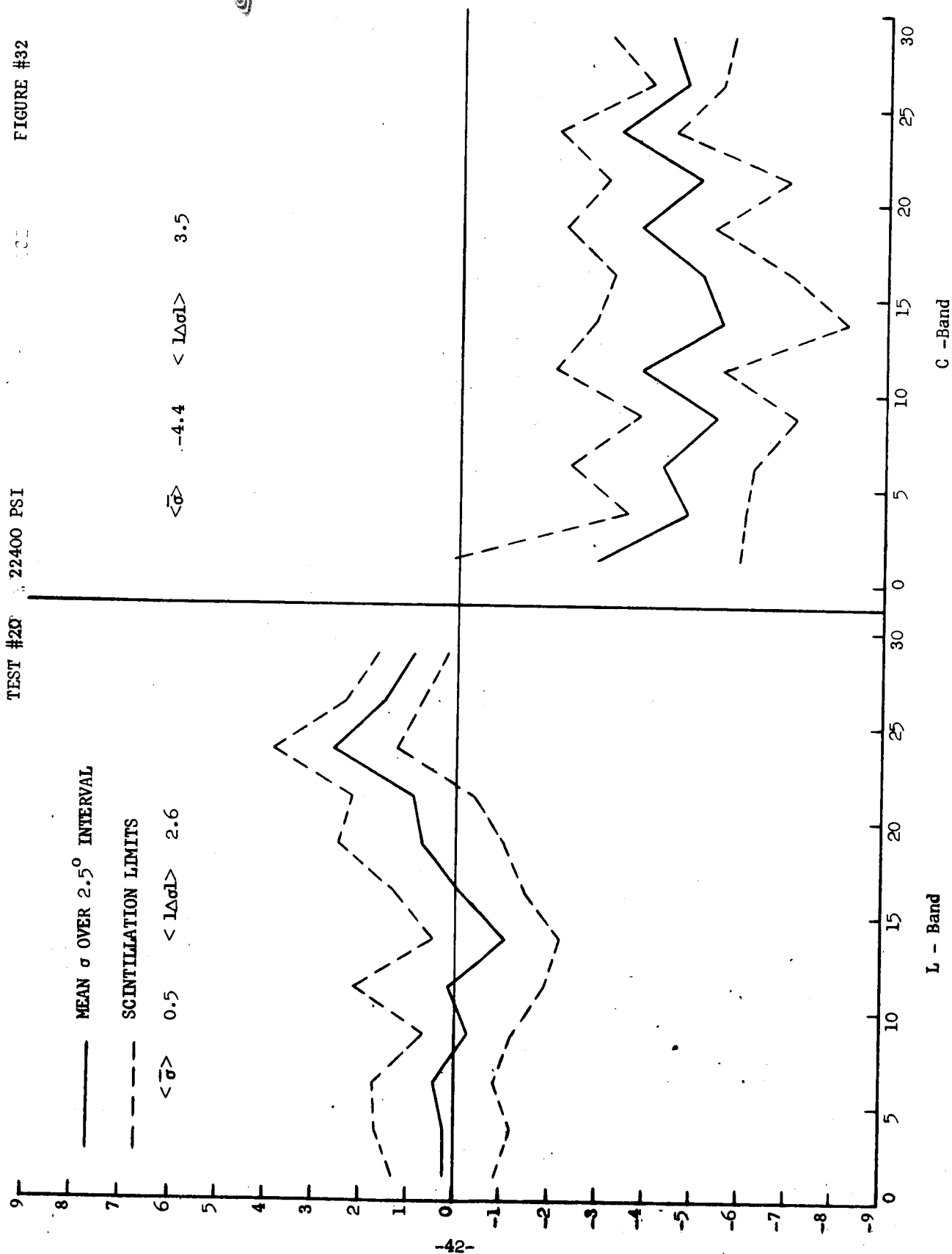




FIGURE #33

0 - 2.5° L Band

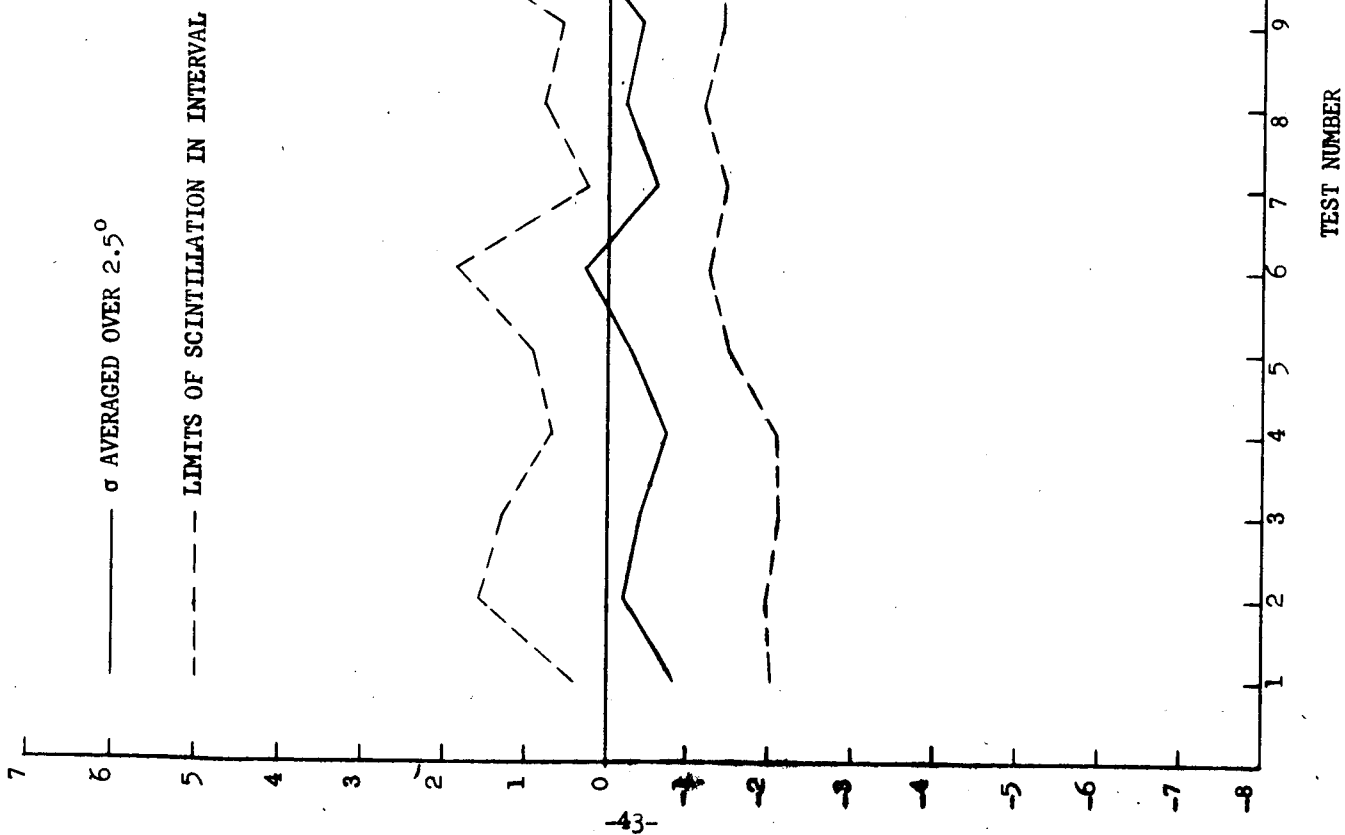
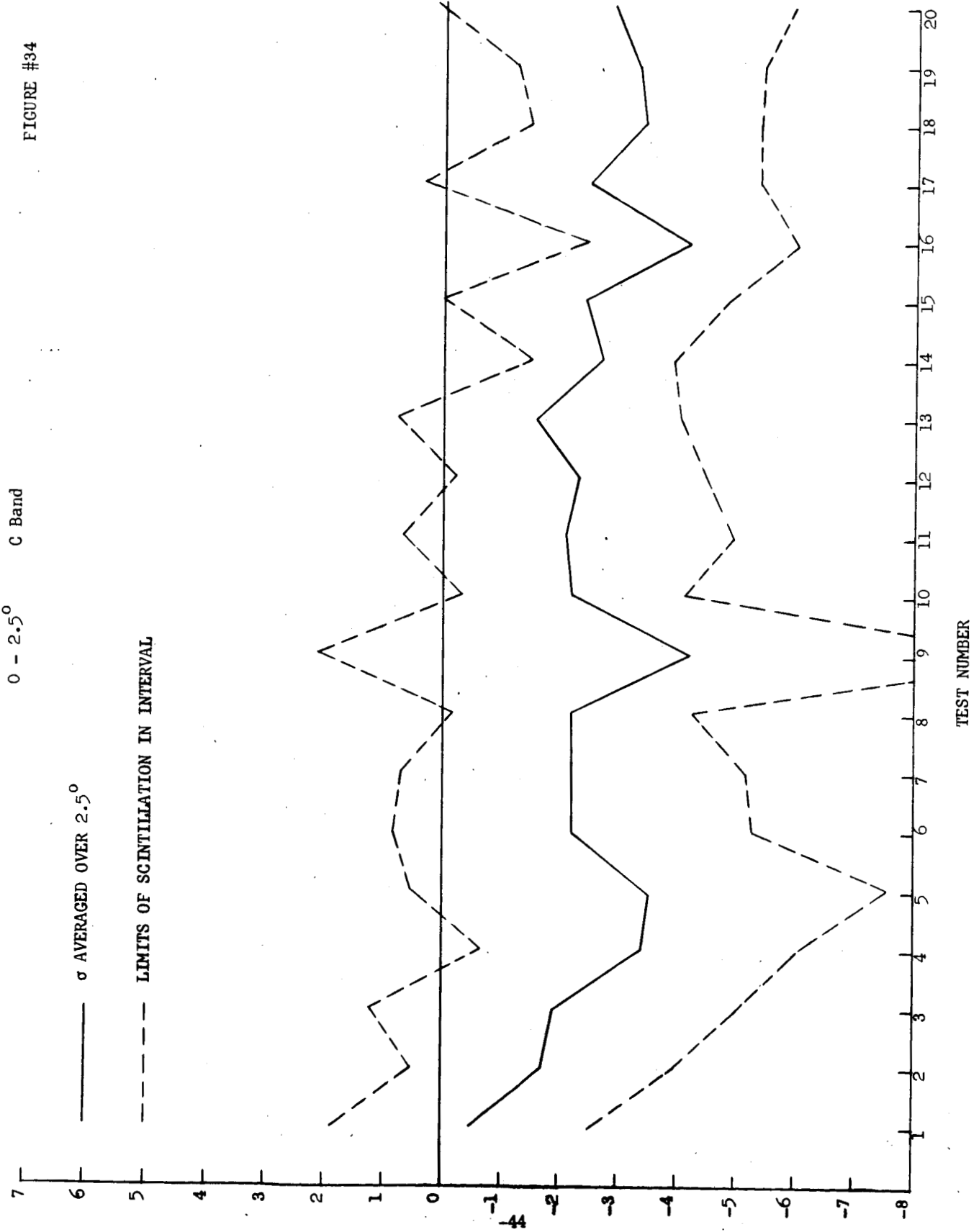


FIGURE #34



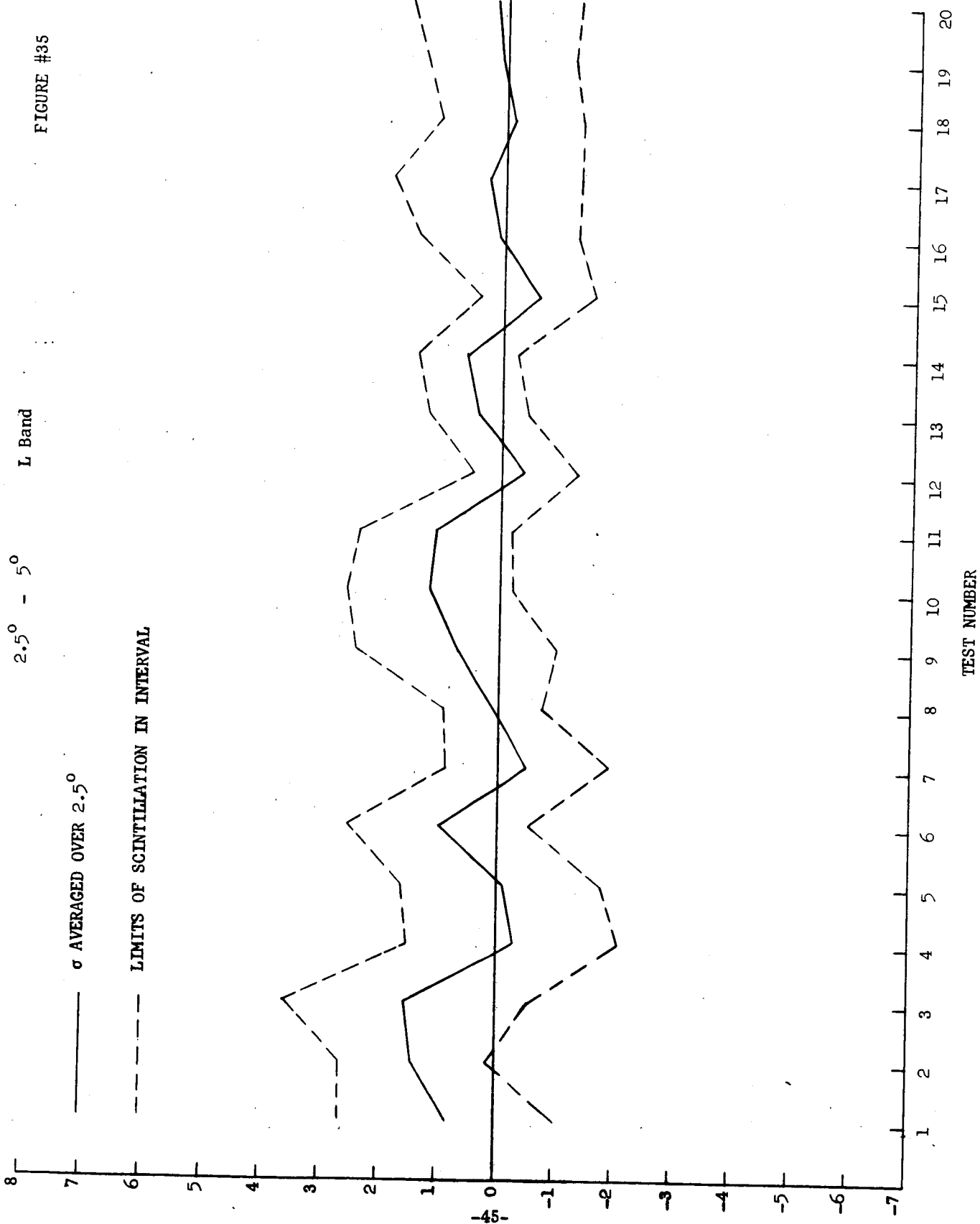


FIGURE #36

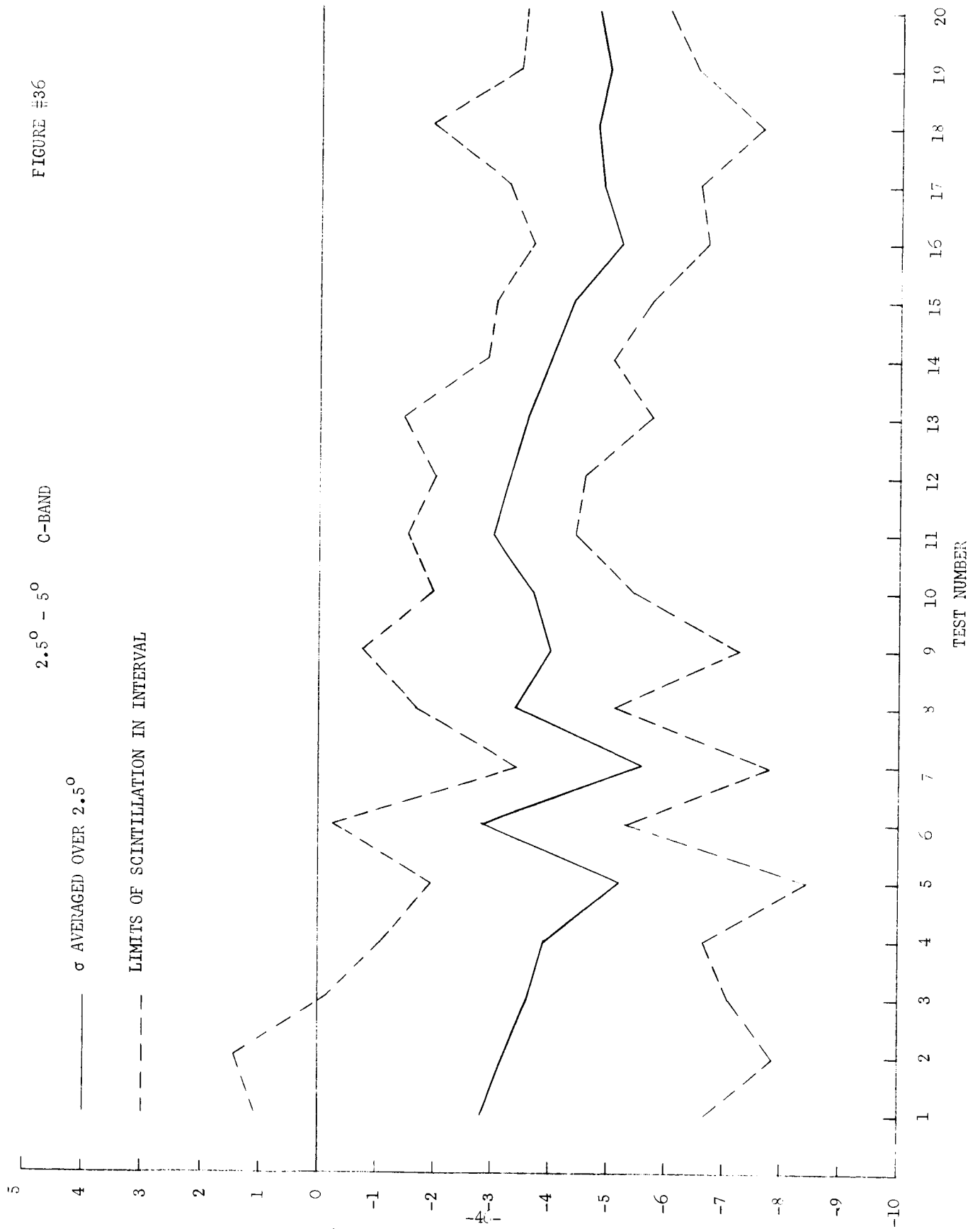


FIGURE #37

5° - 7.5° L-BAND

$\sigma$  AVERAGED OVER 2.5°

LIMITS OF SCINTILLATION IN INTERVAL

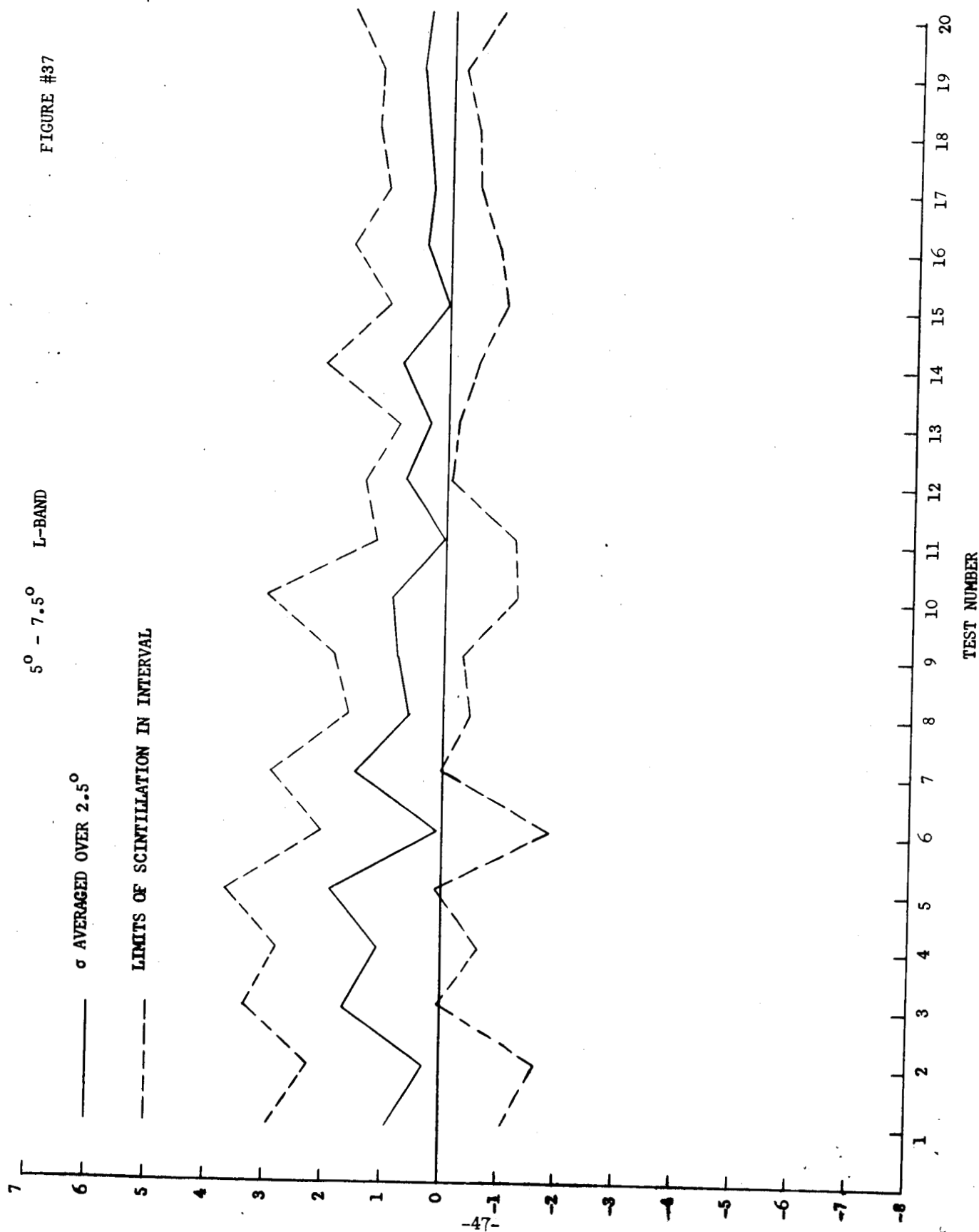


FIGURE #38

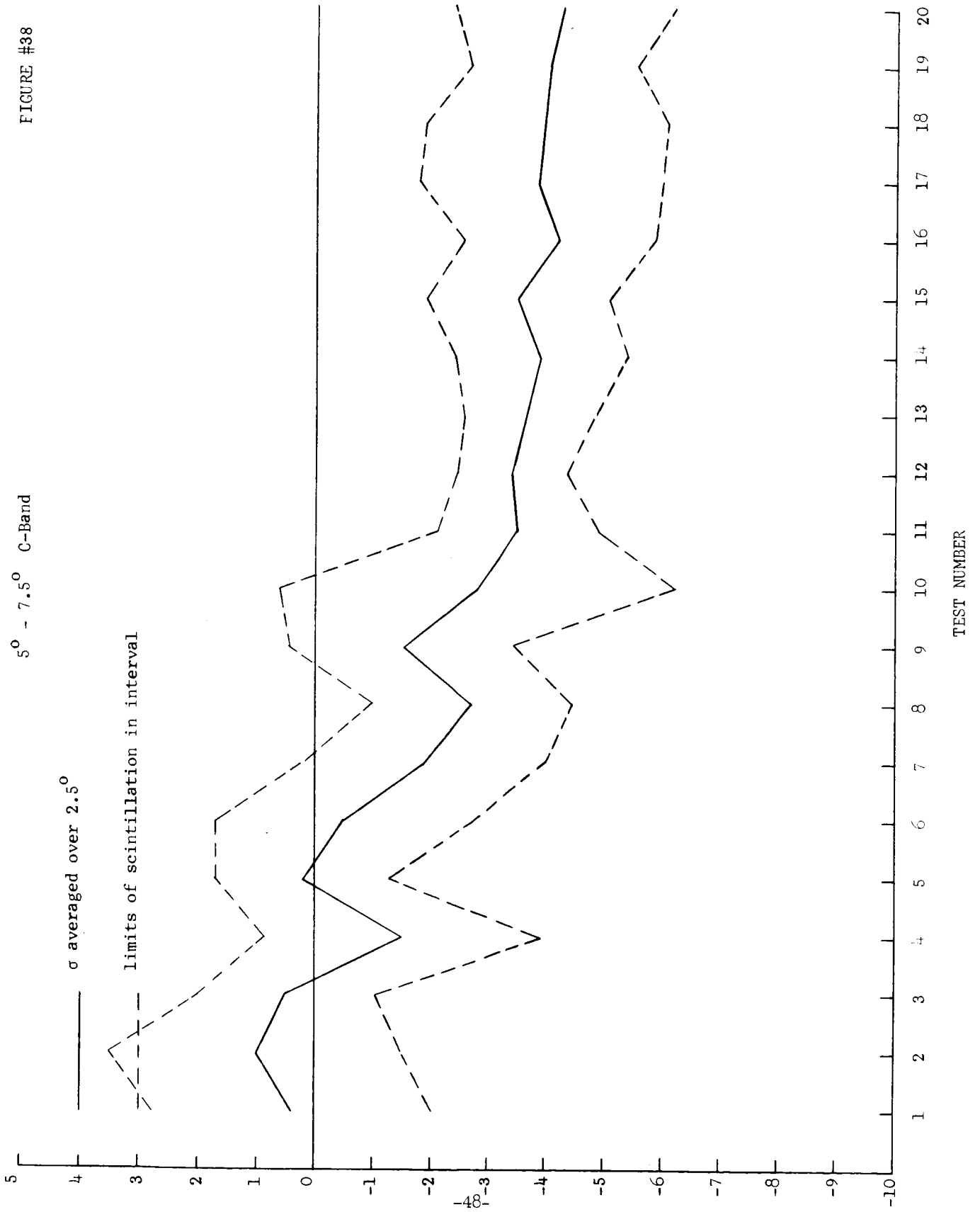


FIGURE #39

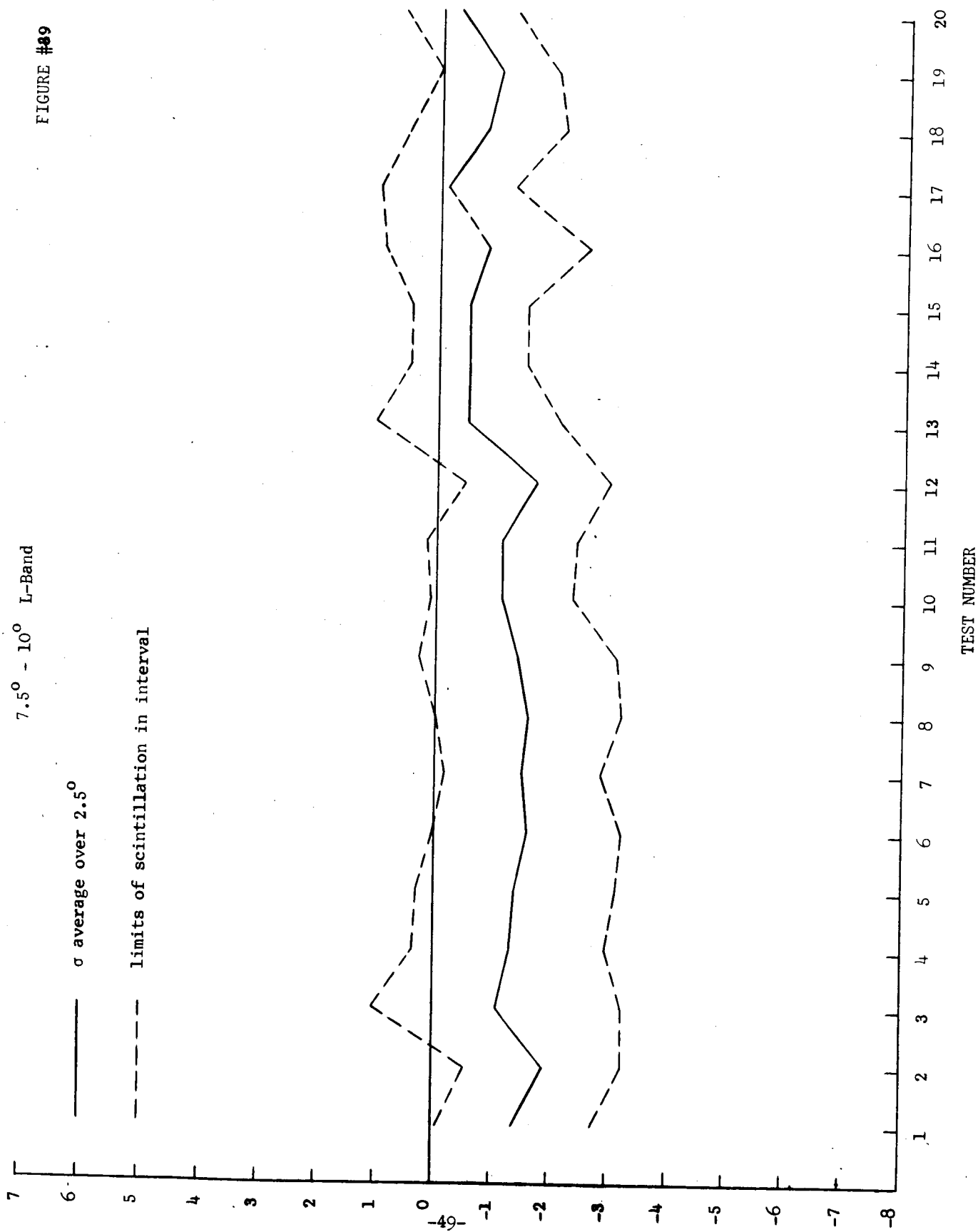
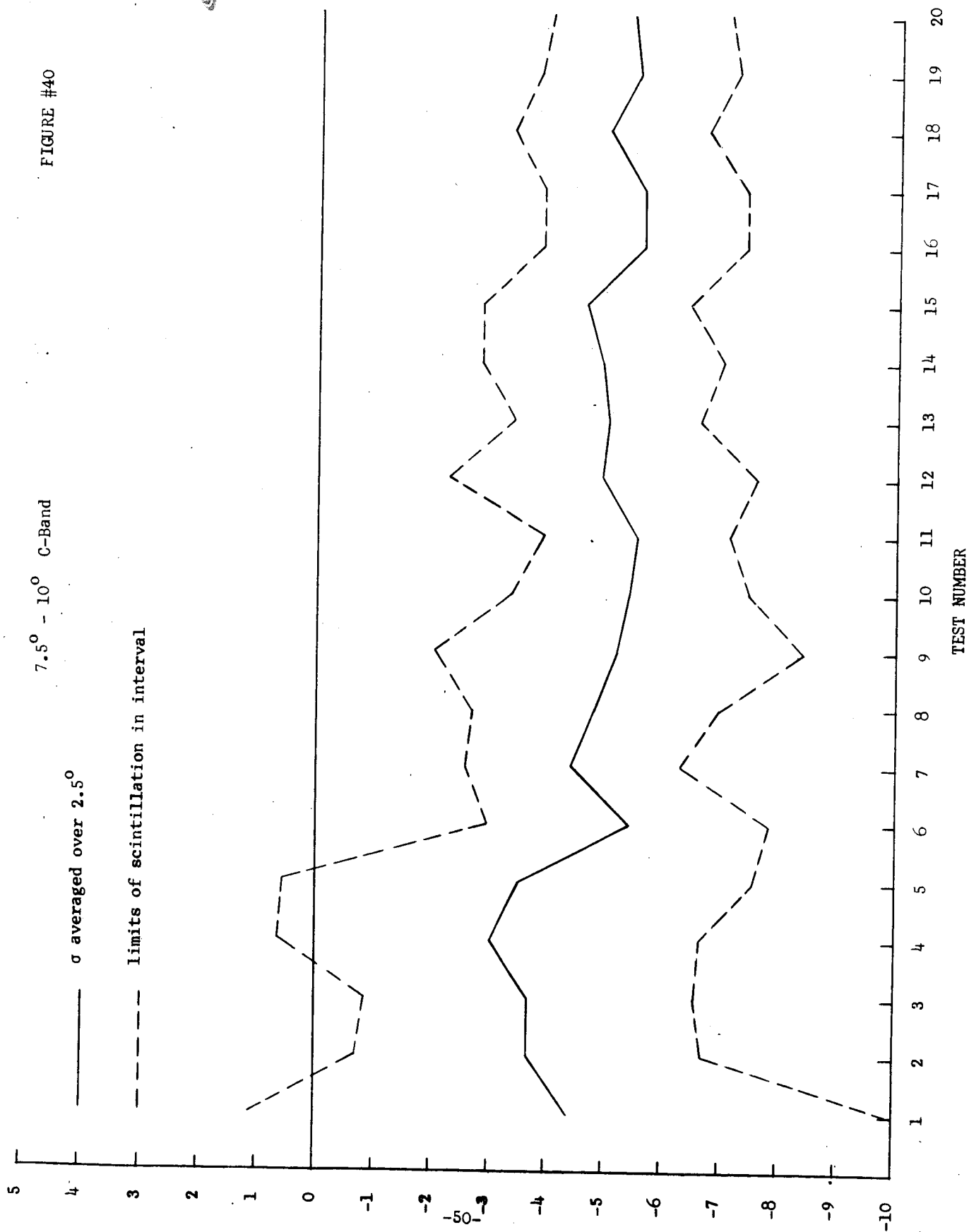


FIGURE #40





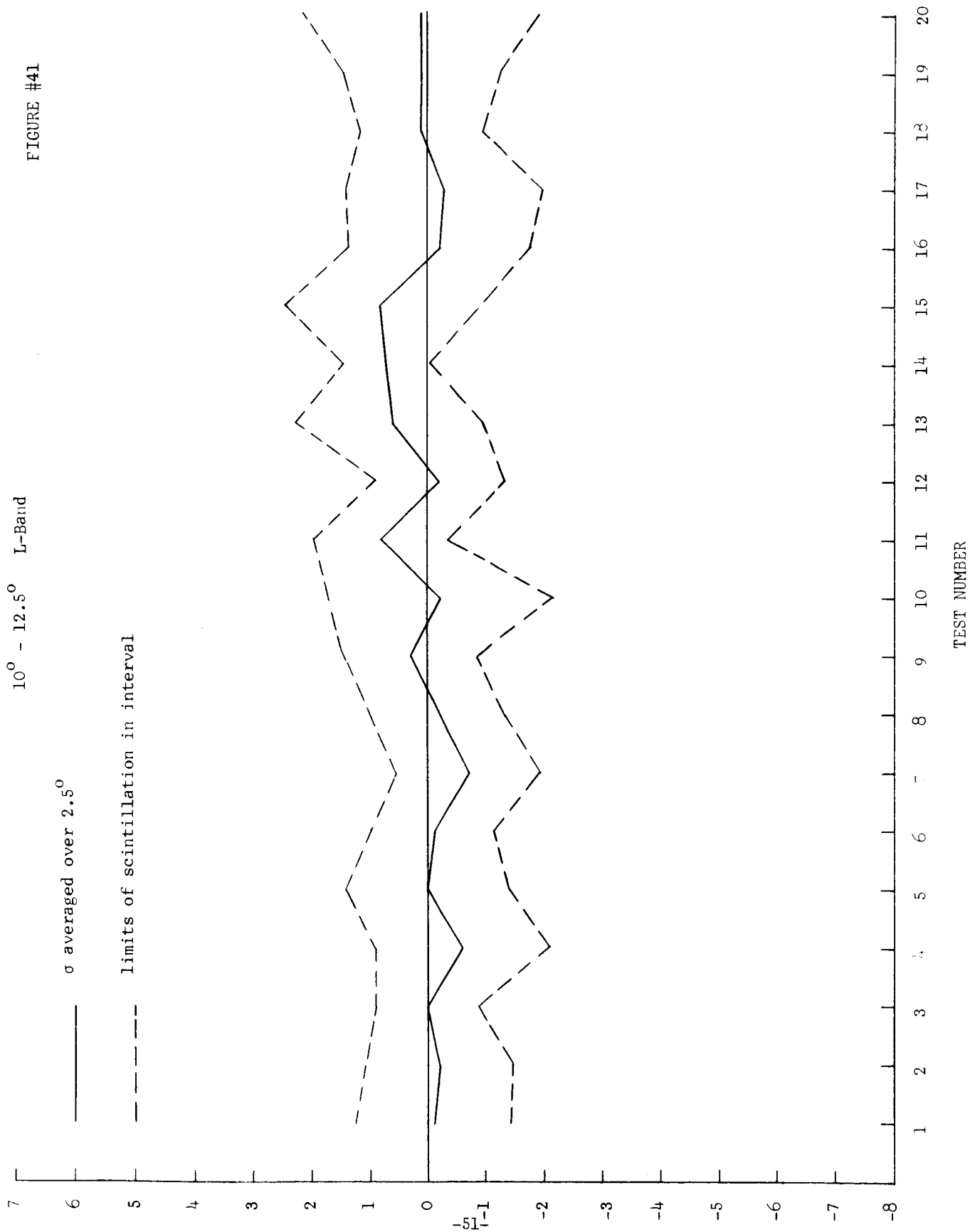


FIGURE #42

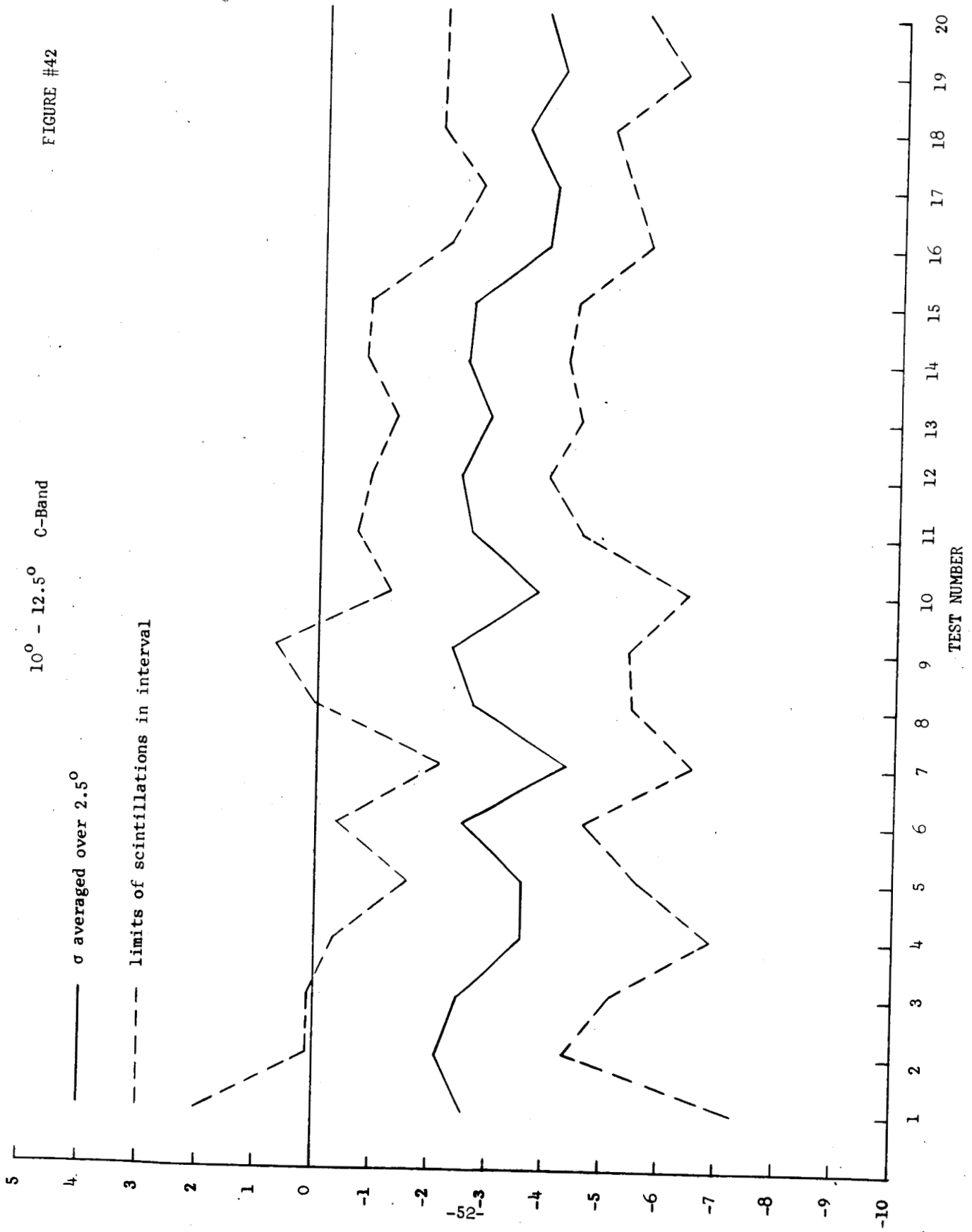


FIGURE #43

12.5° - 15° L-Band

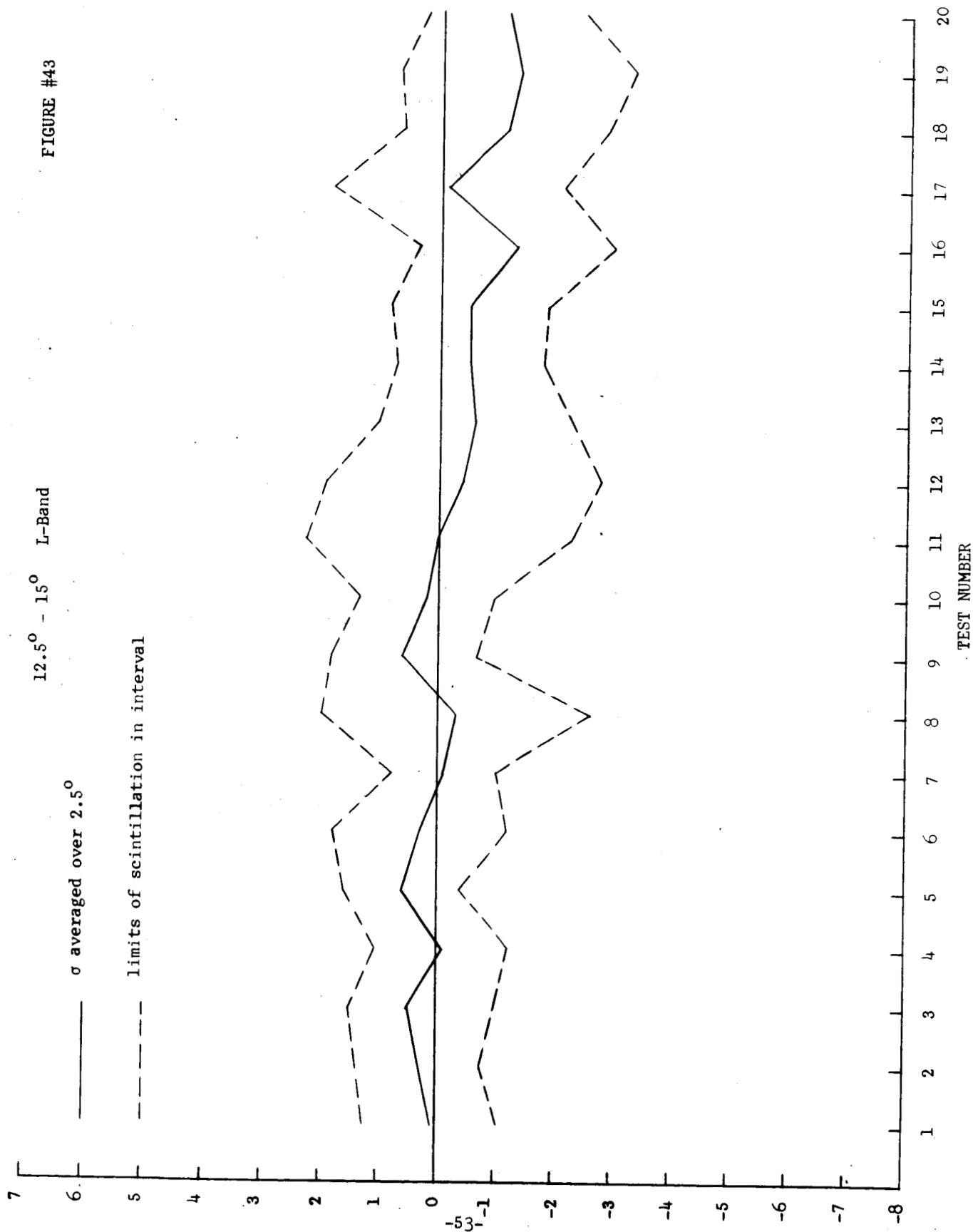
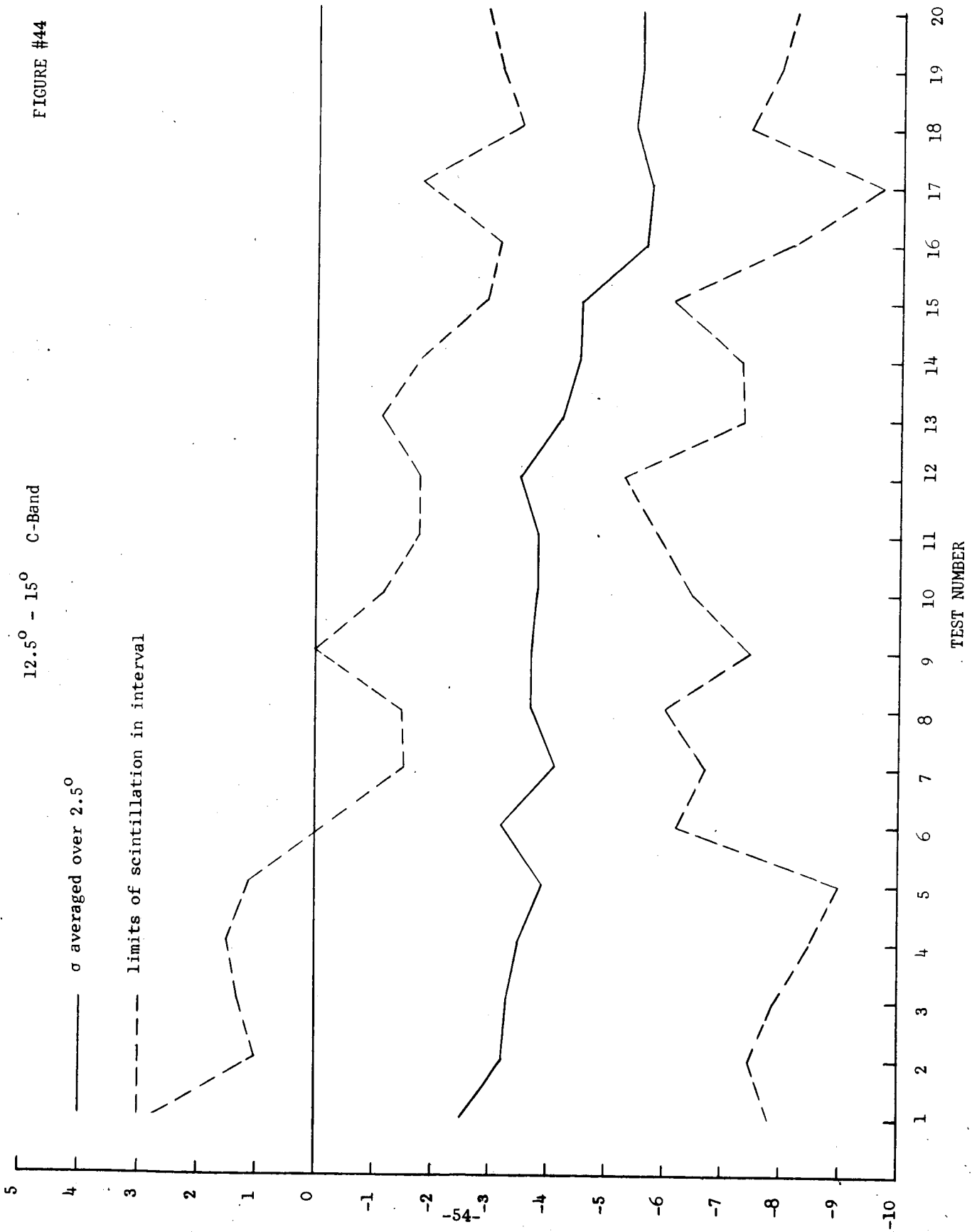


FIGURE #44



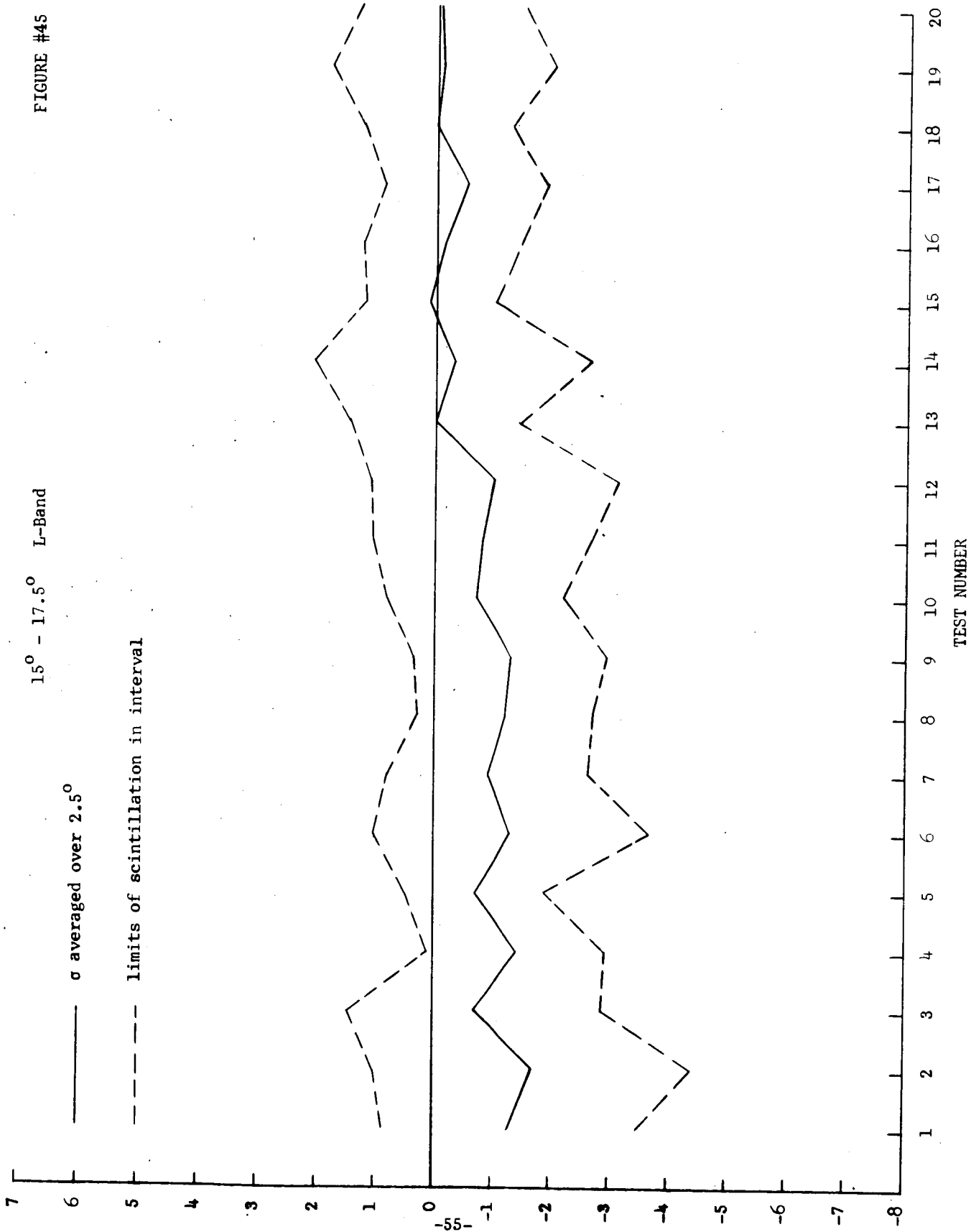
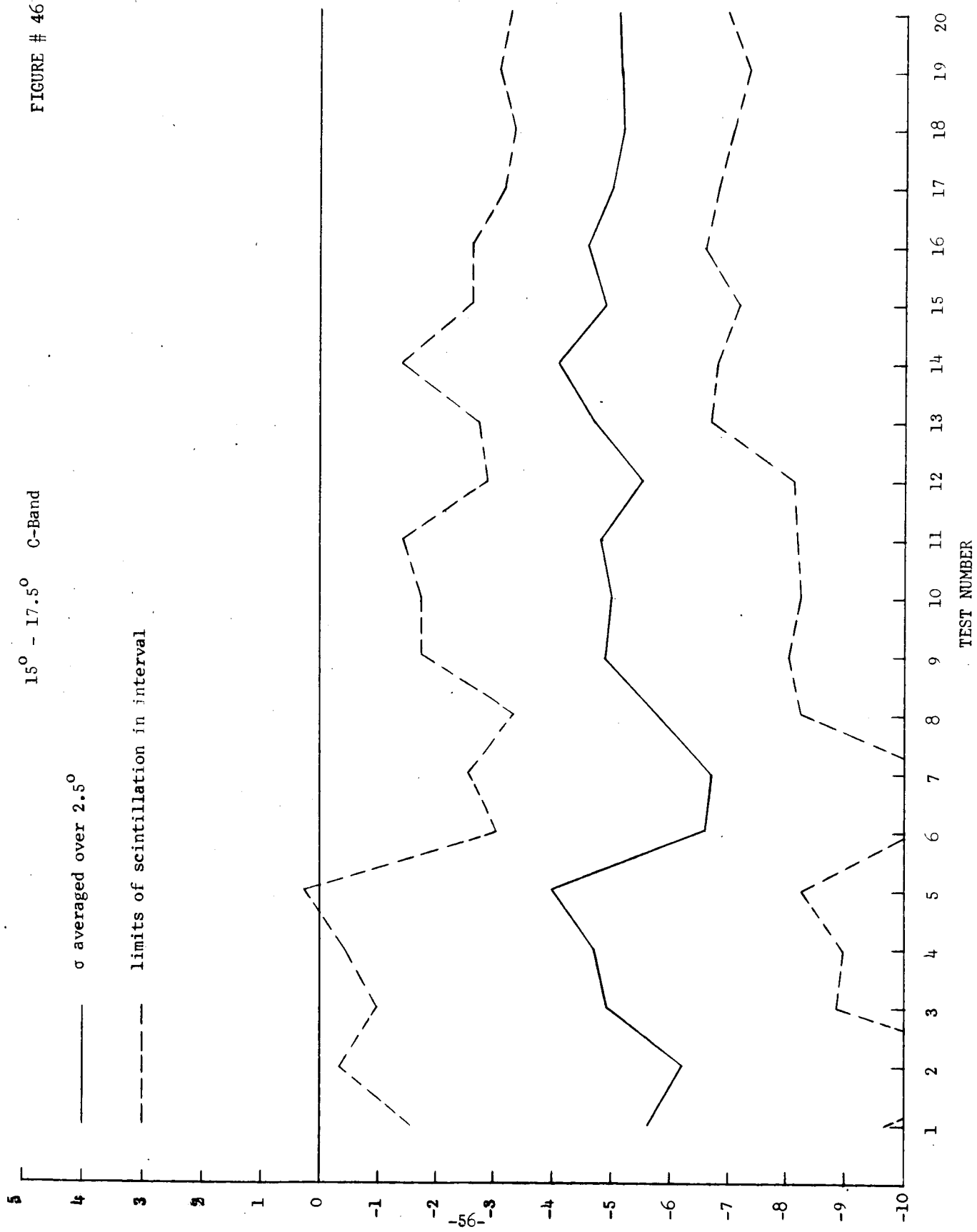


FIGURE # 46



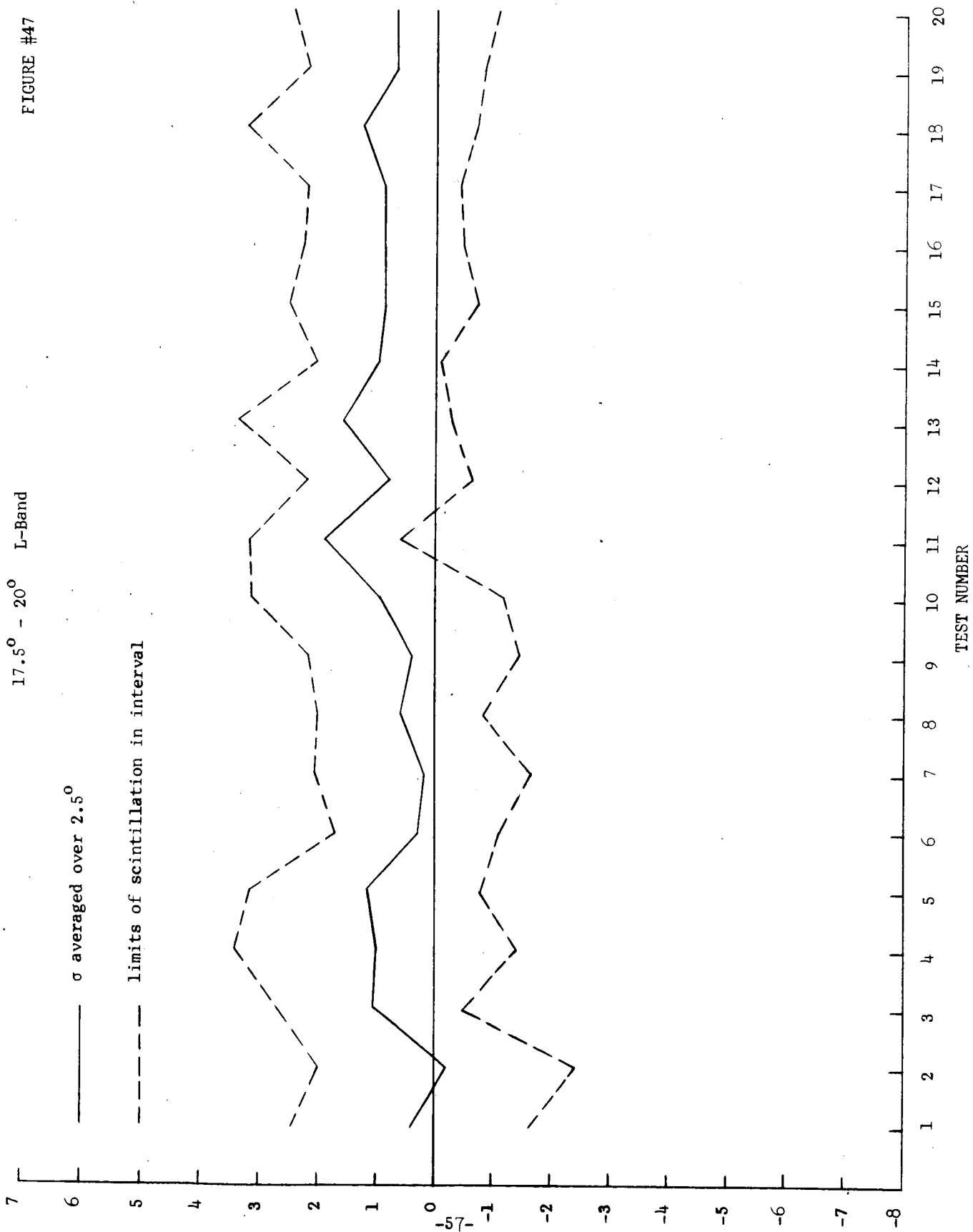


FIGURE #48

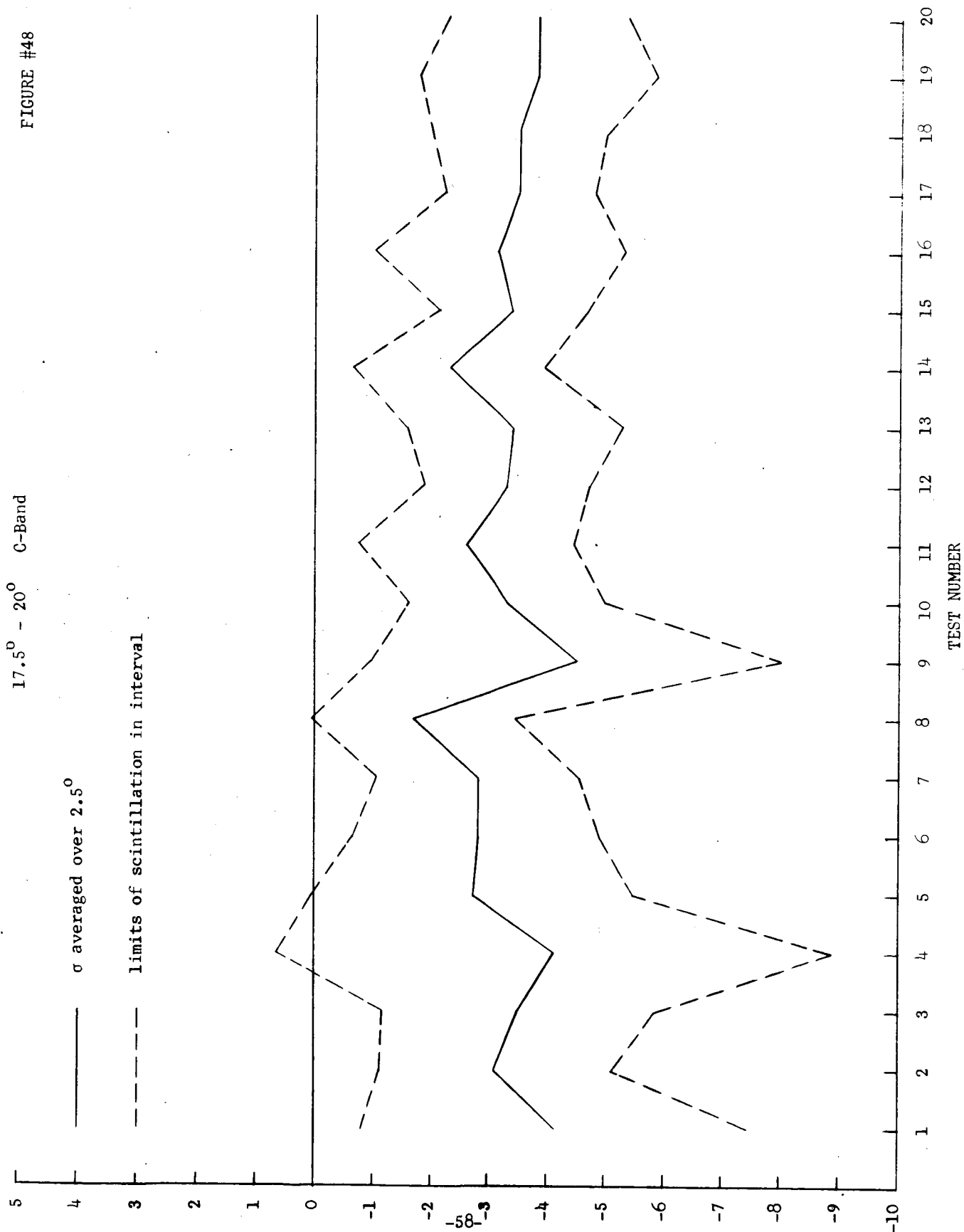




FIGURE #49

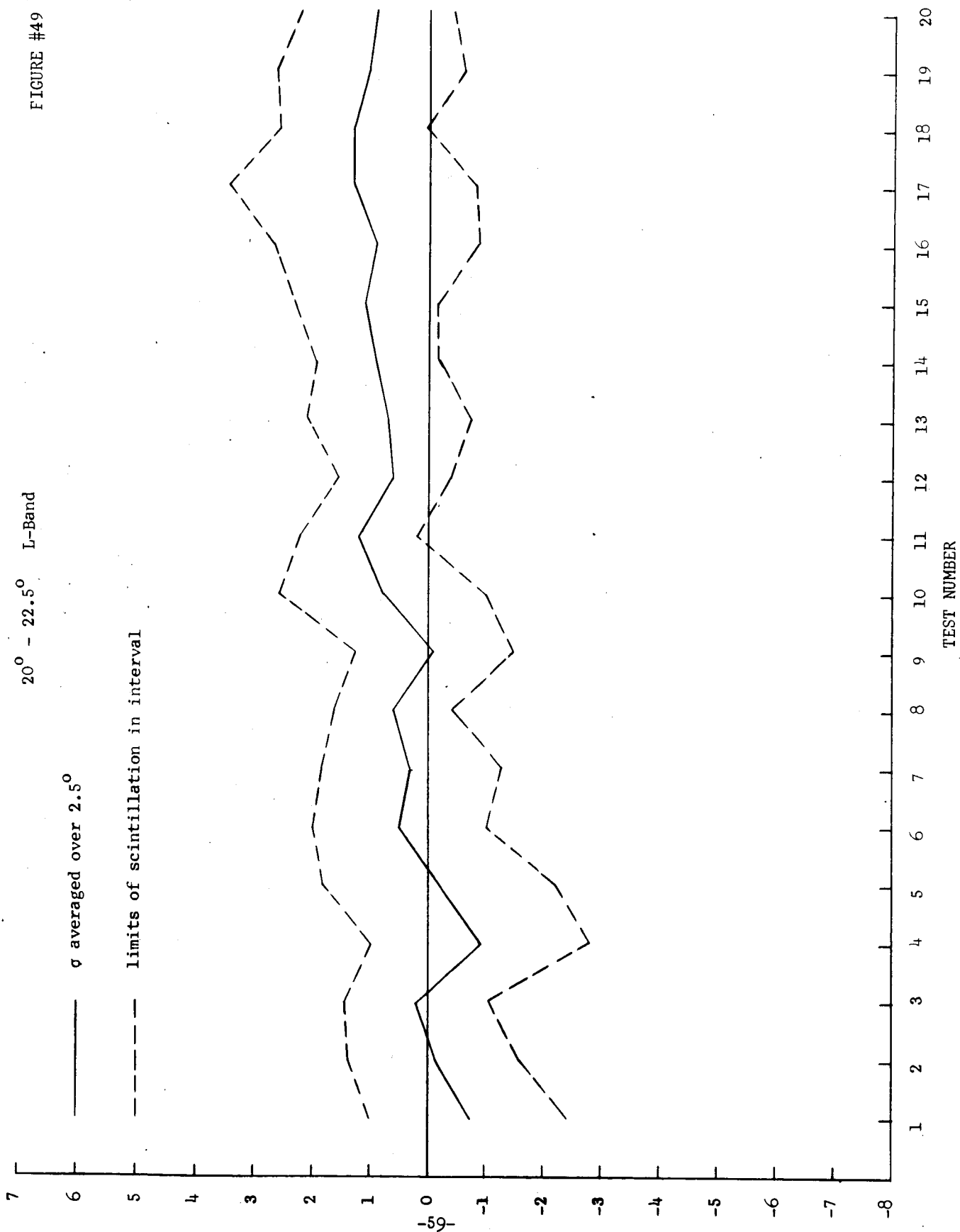
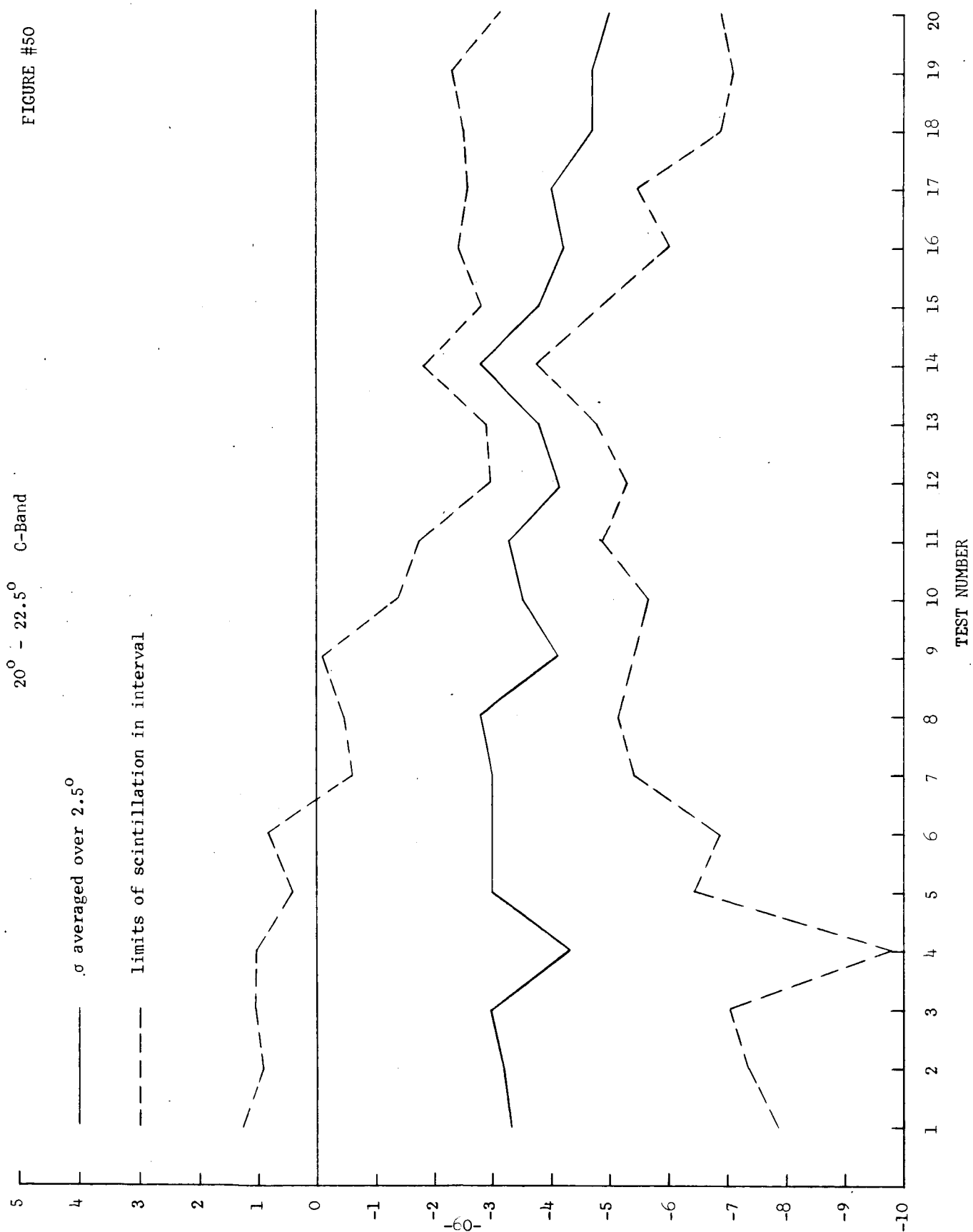


FIGURE #50



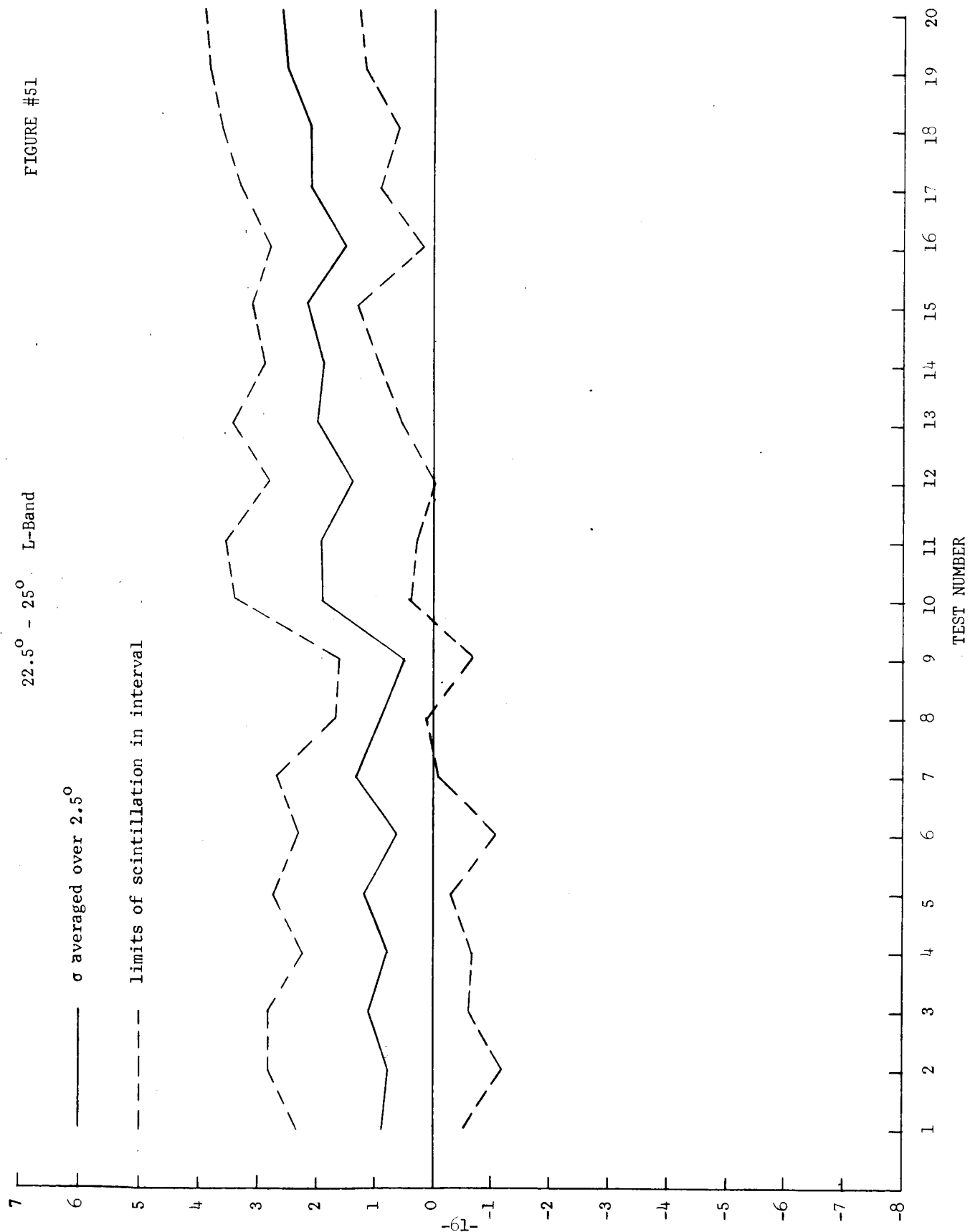
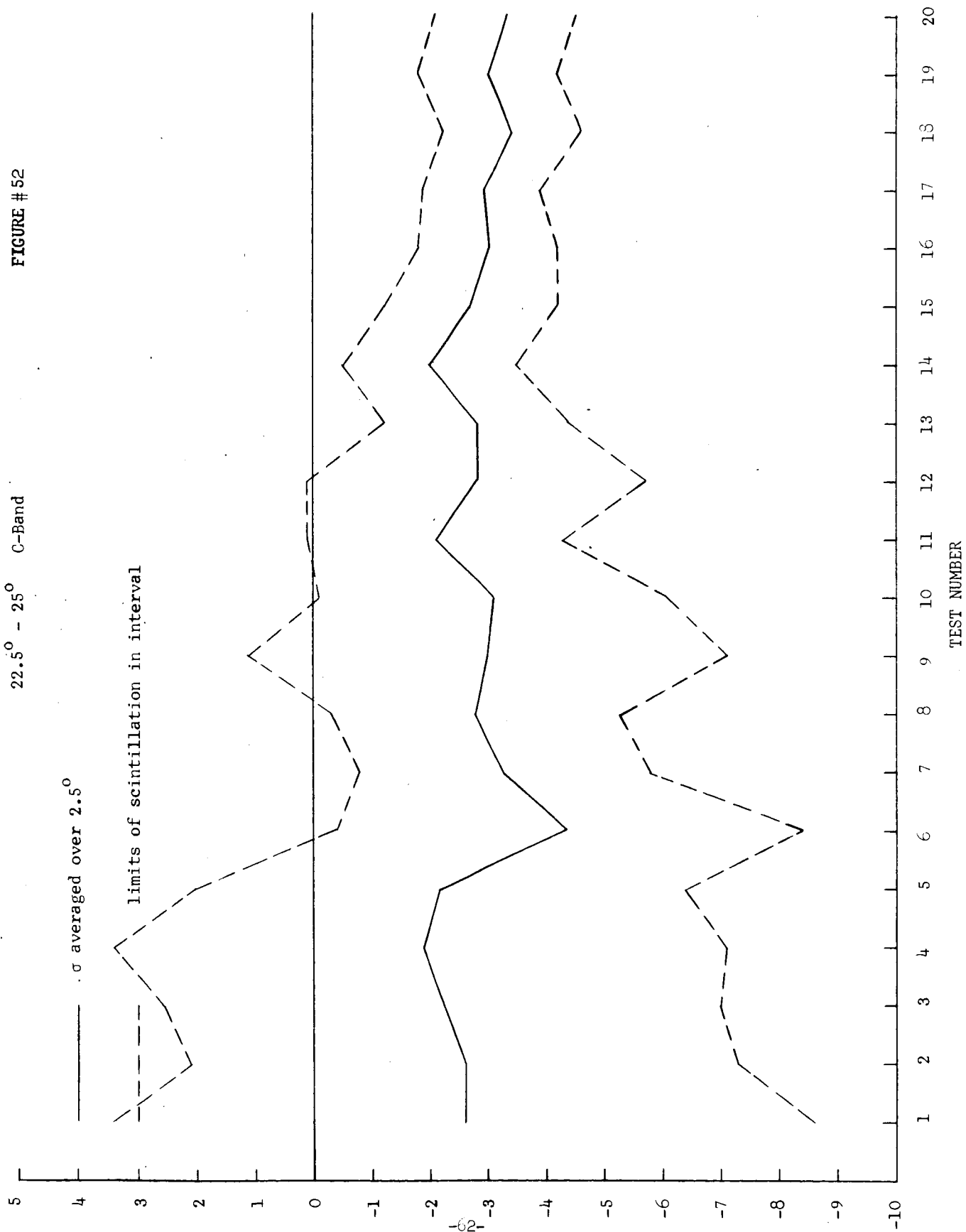


FIGURE # 52

22.5° - 25° C-Band



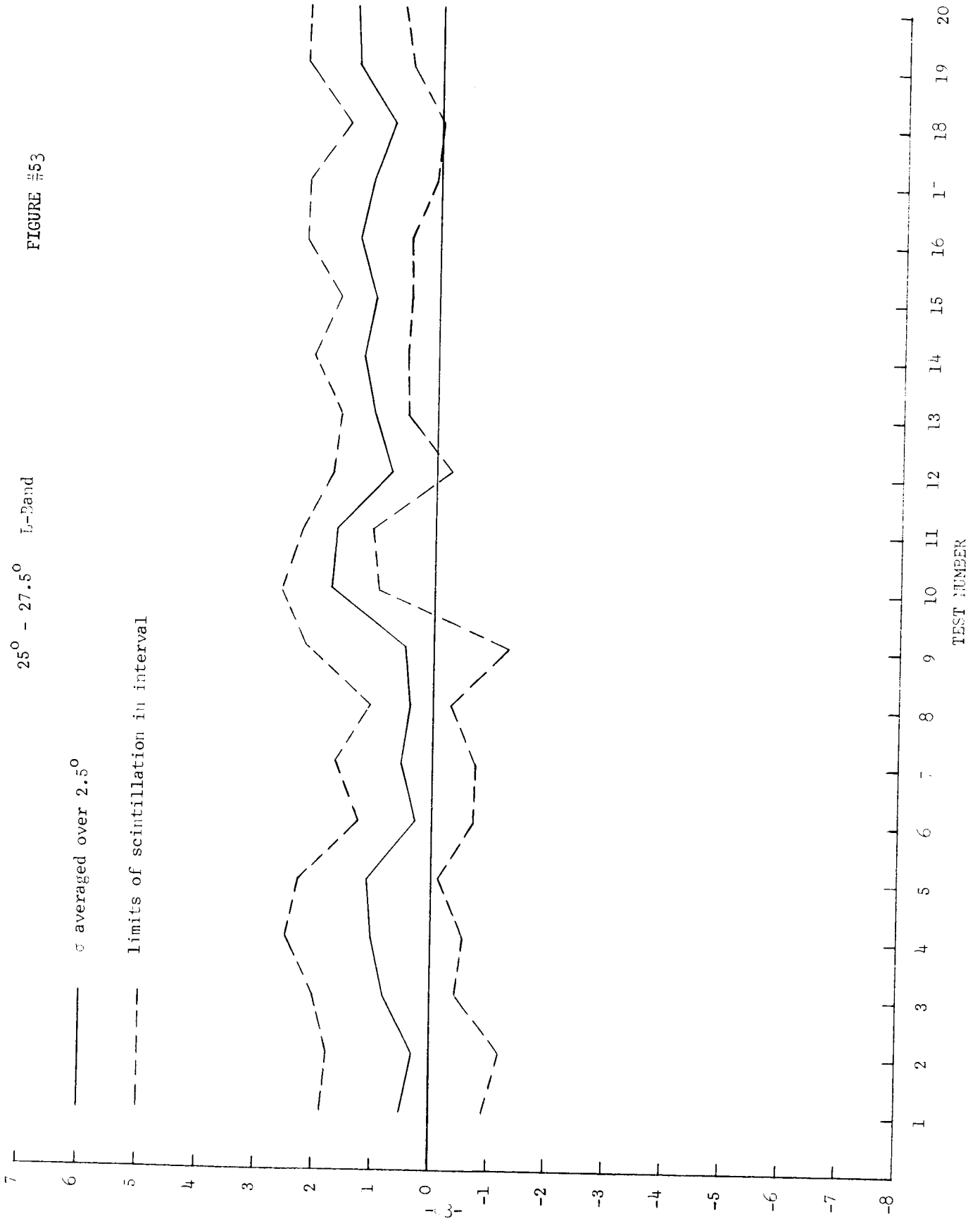
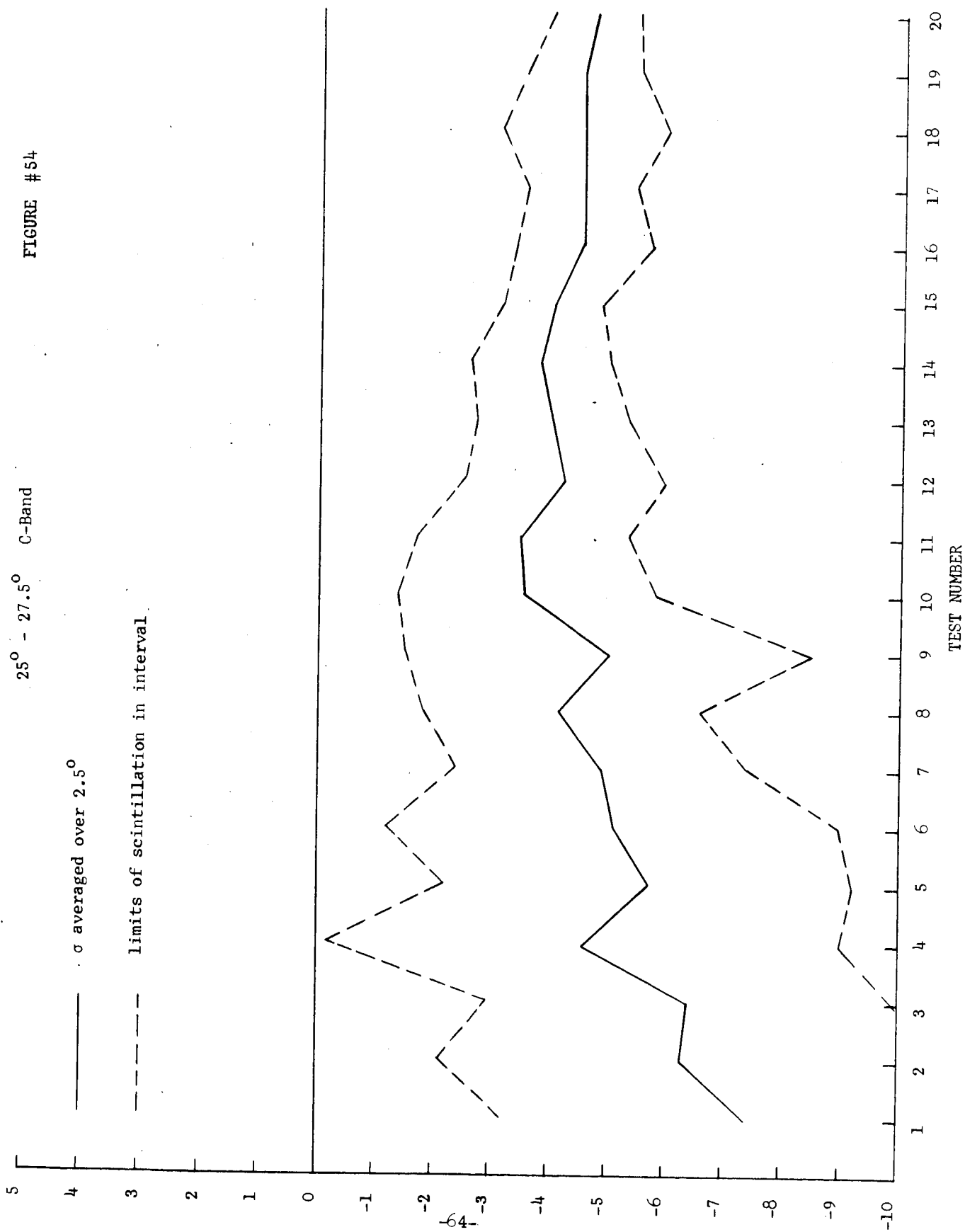
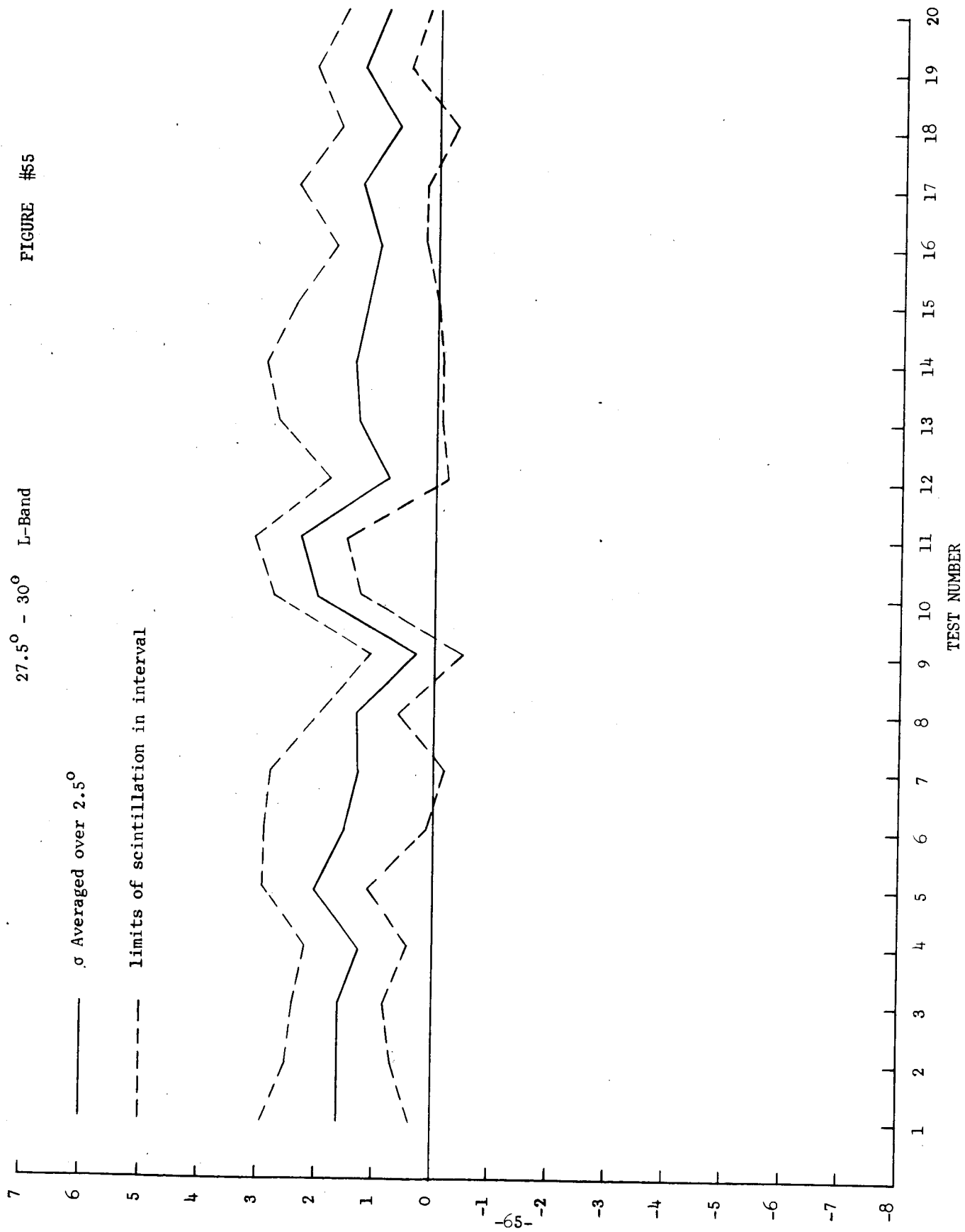
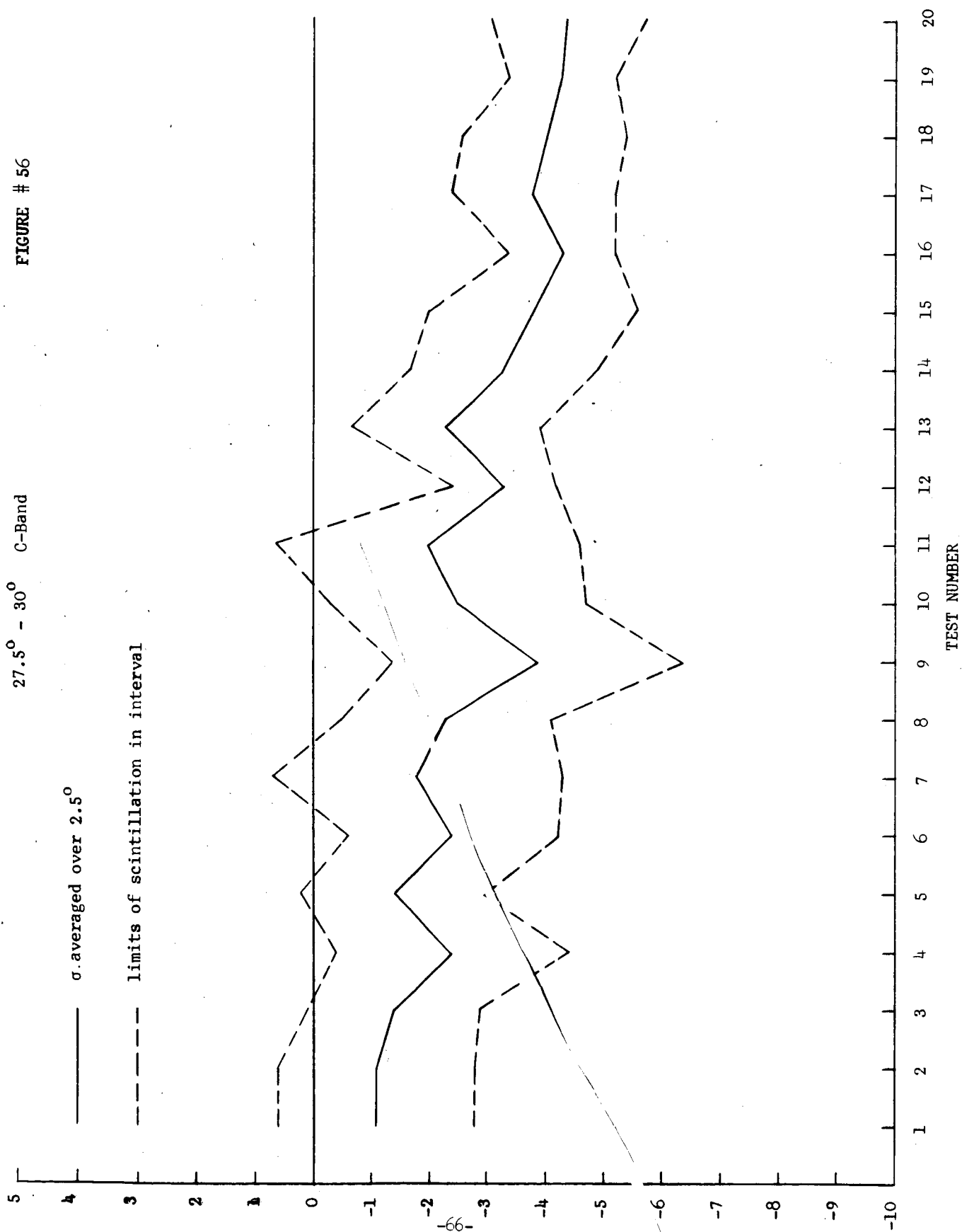


FIGURE #54

25° - 27.5° C-Band









L B A N D

